

EFFECTS OF DEOXYGENATION IN SICKLE CELL ANEMIA

By

DAVID G. MORIO

A THESIS PRESENTED TO THE GRADUATE SCHOOL  
OF THE UNIVERSITY OF FLORIDA IN PARTIAL FULFILLMENT  
OF THE REQUIREMENTS FOR THE DEGREE OF  
MASTER OF SCIENCE

UNIVERSITY OF FLORIDA

AUGUST 1996

Copyright 1996

by

DAVID G. MORIO

## ACKNOWLEDGMENTS

I wish to express my sincere gratitude to Dr. Roger Tran-Son-Tay for having trust in me during these two years and would like to thank him for his many suggestions.

My appreciation also goes to Dr. R.J. Hirko and Dr. U.H. Kurzweg for serving on my committee.

For their assistance in the completion of this work, I am indebted to R. Brown, Dr. A.N. Schechter, MD, Dr. C.T. Noguchi, PhD, Dr. Y.J. He, MD. I also wish to extend my gratitude to Dr. R. Lottenberg, MD, and his staff for providing blood samples from their sickle cell clinic.

Most importantly, I would like to thank my friends and labmates, Manue, Neal, HCK, Luis and of course Philou, for making these two years spent in the lab, great memories.

This work was supported by the National Institutes of Health through grant 7 RO1 HL 49060.

## TABLE OF CONTENTS

ACKNOWLEDGMENTS.....	iii
LIST OF TABLES.....	vi
LIST OF FIGURES.....	vii
INTRODUCTION AND BACKGROUND.....	1
1.1. Introduction.....	1
1.2. Objectives.....	2
1.3. Background.....	4
1.4. Significance.....	12
MATERIALS AND METHODS.....	15
2.1. Instrumentation.....	15
2.1.1. Microrheometer Chamber.....	15
2.1.2. Time-to-Voltage Conversion.....	18
2.1.3. Data Acquisition.....	21
2.1.4. Controls of Partial Pressure in Oxygen and Oxygen Saturation.....	24
2.2. Experiments at 37°C and Various PO <sub>2</sub> .....	27
2.2.1. Speed of Sound.....	27
2.2.2. Steady-State Viscosity Measurement.....	28
2.3. Calibration.....	31
2.4. Blood Preparation.....	33
2.5. Hemoglobin Solution Preparation.....	34
2.6. Determination of Polymer Fraction.....	35
THEORY.....	37
3.1. Speed of Sound.....	37
3.2. Steady-State Viscosity.....	39
RESULTS.....	42
4.1. Blood Analysis.....	42
4.2. Red Blood Cell Suspensions in Plasma.....	49
4.3. Red Blood Cell Suspensions in Phosphate Buffer Solution.....	53
4.4. Hemoglobin Solutions in Plasma.....	57
DISCUSSION.....	61
5.1. Blood Analysis.....	61
5.2. Study of Deoxygenation on Cell Rheology.....	62
5.3. Further Work.....	65
LIST OF REFERENCES.....	79
BIOGRAPHICAL SKETCH.....	83



LIST OF TABLES

<u>Table</u>	<u>page</u>
2.1: Viscosity Measurements of Normal and Sickle Red Blood Cell Suspensions.....	33
4.1: Hemoglobin Electrophoresis Results.....	43
4.2: Complete Blood Count Results.....	44
4.3: Hemoglobin Electrophoresis and MCHC Summary.....	47

LIST OF FIGURES

<u>Figure</u>	<u>page</u>
1.1: Typical Shapes for Normal (AA) and Sickle (SS) Red Blood Cells.....	5
1.2: Dissociation Curve - Relationship between the Partial Pressure in Oxygen and the Saturation in Oxygen.....	7
2.1: Microrheometer Schematic.....	16
2.2: Simplified TVC Block Diagram.....	19
2.3: Time-to-Voltage Converter Setup.....	20
2.4: Typical TVC Measure.....	22
2.5: Controls of Partial Pressure in Oxygen and Oxygen Saturation.....	25
2.6: Characteristic Curve for a Polarographic Oxygen Electrode.....	27
2.7: Typical Output for a Falling Ball Experiment.....	30
2.8: Speed of Sound in Distilled Water as a Function of Temperature.....	32
3.1: Falling Ball in a (a) Unbounded Fluid and (b) Cylindrical Tube.....	39
4.1: Polymer Fraction Profiles: donors 1 to 5 (AS) and donors 6 to 10 (SS).....	48
4.2: Apparent Viscosity vs. PO <sub>2</sub> : (a) AA donors, (b) AS donors, and (c) SS donors.....	50
4.3: Apparent Viscosity vs. SO <sub>2</sub> : (a) AA donors, (b) AS donors, and (c) SS donors.....	51
4.4: Apparent Viscosity vs. Polymer Fraction: (a) AA donors, (b) AS donors, and (c) SS donors.....	52
4.5: Apparent Viscosity vs. PO <sub>2</sub> : (a) AA donors, (b) AS donors, and (c) SS donors.....	54
4.6: Apparent Viscosity vs. SO <sub>2</sub> : (a) AA donors, (b) AS donors, and (c) SS donors.....	55

4.7: Apparent Viscosity vs. Polymer Fraction: (a) AA donors, (b) AS donors, and (c) SS donors.....	56
4.8: Apparent Viscosity vs. PO <sub>2</sub> : (a) AA donors, (AS) donors, and (SS) donors.....	58
4.9: Apparent Viscosity vs. SO <sub>2</sub> : (a) AA donors, (b) AS donors, and (c) SS donors.....	59
4.10: Apparent Viscosity vs. Polymer Fraction: (a) AA donors, (b) AS donors, and (c) SS donors.....	60
5.1: Best Curve Fits: Apparent Viscosity vs. Polymer Fraction (a) RBC in Plasma, (b) RBC in PBS, and (c) Hb in Plasma.....	66
5.1: Best Curve Fit: Apparent Viscosity vs. Polymer Fraction: SS, AS RBC in Plasma and PBS.....	67



Abstract of Thesis Presented to the Graduate School  
of the University of Florida in Partial Fulfillment of the  
Requirements for the Degree of Master of Science

EFFECTS OF DEOXYGENATION IN SICKLE CELL ANEMIA

By

DAVID G. MORIO

August, 1996

Chairman: Roger Tran-Son-Tay  
Major Department: Aerospace Engineering, Mechanics, and Engineering  
Science

Sickle cell anemia is a disease that affects the rheological properties of red blood cells. A ball microrheometer has been developed in this laboratory to measure the rheological properties of very small quantities (20  $\mu$ l) of sickle red blood cell suspensions. The effects of steady deoxygenation at "equilibrium" on the rheological properties of sickle red blood cells resuspended at 25 % hematocrit in autologous plasma and in Phosphate Buffer Solution are measured. Hemoglobin solutions at 25 % hematocrit in autologous plasma, obtained by sonication, are also studied. To separate the effects of membrane abnormalities from that of the hemoglobin S polymer, sickle trait and sickle cell blood are used. Sickle trait red blood cells have minimal membrane abnormalities and their population exhibit a minimal density heterogeneity.

Rheological properties are characterized as a function of partial pressure in oxygen, oxygen saturation, and polymer fraction. No apparent correlation is seen when viscosity is plotted as a function of

partial pressure in oxygen or saturation in oxygen. On the other hand, a linear relationship is found between cell suspension viscosity and polymer fraction up to a critical value of 30 % in sickle trait individuals and 55 % in sickle cell patients. Above this critical value of 55 %, a sharp increase in viscosity in sickle cell patients is seen. The data for sickle trait and sickle cell blood cells coincide and show that viscosity and polymer fraction are linearly related up to polymer fraction value of 55 %.

This study offers new insight into our understanding and characterization of the rheological properties of sickle red blood cells. It is found that viscosity may be a good parameter for assessing the clinical severity in sickle cell anemia and for evaluating the effects of pharmacological agents.

CHAPTER 1  
INTRODUCTION AND BACKGROUND

1.1. Introduction

Sickle cell anemia (SCA) afflicts Afro-Americans in the United-States, and black people in most South-American, African, and West-Indies countries. In sickle cell disease, sickler patients have red blood cells that are not capable of traversing the capillaries and consequently of delivering oxygen to the nearby tissues, which is one of the main functions of red blood cells. Sickler patients experience numerous pathological complications and frequent vaso-occlusive painful crises. Researchers have been working on sickle cell anemia for more than 30 years now and even if they have made tremendous progress into the characterization of this disease, they still do not have a complete understanding of all its mechanisms. Many treatments have been tested targeting either the hemoglobin, the erythrocytes or the gene (Hydroxyurea, drugs increasing the oxygen affinity, etc.) [Rodgers et al., 1994]. None of them can be considered as the final remedy to sickle cell anemia yet. Rheological studies offer a means to characterize the sickling process, which is believed to be the dominant factor in SCA.

The system used for the present study is a newly designed magneto-acoustic ball microrheometer, originally developed by Tran-Son-Tay et al. [1988], that allows viscoelastic measurements of any fluid. Its main advantages are requirement of a very small sample volume (20  $\mu$ l)

and the capability of studying translucent as well as opaque solutions. Because the sample volume required is so small, temperature is accurately and rapidly controlled. The most common rheometers are based on the measurement of stress on a fixed surface while a parallel surface is moved with a known applied strain. Cone/plate viscometers (model RVTDCP, Wells-Brookfield, Massachusetts) rotate a conical spindle at a fixed and accurately controlled speed and measures precisely the steady-state viscosity of any fluids within the range (32 cP to 196600 cP). As another example, couette viscometers can be operated in constant as well as in oscillatory modes and provide accurate viscoelastic measurement [Gilinson et al., 1963; Tran-Son-Tay et al., 1986]. Those two systems require a larger sample volume of at least 2 ml. Optical technique is also being used to develop new kind of rheometers, but limiting their measurements to translucent solutions only [Ziemann et al., 1994].

The ball microrheometer employs a tiny stainless steel ball that is located in a small, vertical capillary tube, held by a temperature controlled Lexan<sup>TM</sup> water jacket. The motions of the ball are tracked using an ultrasonic technique, associated with a Time-to-Voltage Conversion technique. Steady-state viscosity and complex viscosity (viscous component,  $\eta'$ , and elastic component,  $G'$ ) are measured by applying a known force on the ball surrounded by a fluid located in the glass capillary tube.

## 1.2. Objectives

The purpose of this study is to understand and characterize the rheological properties of sickle red blood cells, while varying continuously the oxygen tension. Eventually, the final objective is to

show if there is any correlation between the steady-state viscosity of sickle red blood cell suspensions upon steady deoxygenation, and polymer fraction. Sickle trait (AS) and sickle cell (SS) red blood cells resuspended at 25 % hematocrit will be used in this study. Sickle trait blood was used, because its red blood cells present minimal membrane abnormalities and minimal cell density heterogeneity. Normal red blood cells (AA) also resuspended at 25 % hematocrit will be run as control. All the red blood cell suspensions will be resuspended both in their autologous plasma and in Phosphate Buffer Solution at the wished hematocrit. Hemoglobin solutions will be obtained by sonication from 25 % hematocrit red blood cell suspensions in autologous plasma. The potential effects of plasma proteins as well as the importance of membrane abnormalities for sickle red blood cells will be carefully examined.

This new approach that tries to relate the polymer fraction to the rheological behavior of sickle red blood cell suspensions will lead to some new discernment in sickle cell anemia.

To achieve those goals, the ball microrheometer had to be greatly redesigned. Firstable, a new technique of Time-to-Voltage Conversion will be used to track the motions of the ball. This technique will replace the high frequency counters and electronic board which used to be in charge of that task. The new system will be calibrated with the same protocol than it was in the past (using silicone oils and distilled water). A code will be written and will have to perform the following functions:

- initialization of the parameters of experiment,
- keep a record of patient's information, viscosity results, experiment information, etc.

- reduce the interaction between the operator and the instruments,
- be as convivial and practical as possible.

To investigate the effects of steady deoxygenation on sickle blood rheology, several pieces of equipment will be used:

- a co-oximeter (measures the saturation in oxygen and total hemoglobin concentration),
- a chemical microsensor (measures the partial pressure in oxygen),
- three flowmeters (measure the flow rate of O<sub>2</sub>, CO<sub>2</sub>, N<sub>2</sub> gases),
- an ultrasonic sonicator (to obtain hemoglobin solutions).

Then,

- a bubbling system,
- a mixer,
- a PO<sub>2</sub> calibration cell (inside oxygen tension controlled),
- a PO<sub>2</sub> sample chamber (inside oxygen tension controlled),

will be built for the study.

### 1.3. Background

Sickle cell anemia is a disease involving abnormal hemoglobin within the erythrocyte. It is characterized by a mutant form of hemoglobin protein. Hemoglobin molecules have four polypeptides chains: two alpha ( $\alpha$ ) and two non-alpha chains. Each chain surrounds an iron porphyrin molecule that can reversibly bind oxygen. Usually, the non- $\alpha$  chains are the  $\beta$  chains and combine with two  $\alpha$  chains to form normal hemoglobin A (HbAA) [Mackie and Hochmuth, 1990; Briehl and Nikolopoulou, 1993]. Sickle cell hemoglobin (HbSS) differs from normal hemoglobin in one amino-acid change on the  $\beta$  chain. When exposed to low concentrations in oxygen, the mutant hemoglobin forms elongated crystal polymers with a helical fiber structure, that makes the cells become

more rigid. Sickle cell's flexibility and deformability are thus dramatically changed. Physiologically prolonged low concentrations in oxygen can lead to organ damages, organs such as heart, kidneys and brain. Cells with sickle hemoglobin, commonly named "sickle cells" survive at most one month, which causes chronic anemia and then irreversible physiological changes. The formed polymer can deform the erythrocytes twice as much in length and then give a crescent shape to the erythrocytes as shown in Fig. 1.1.

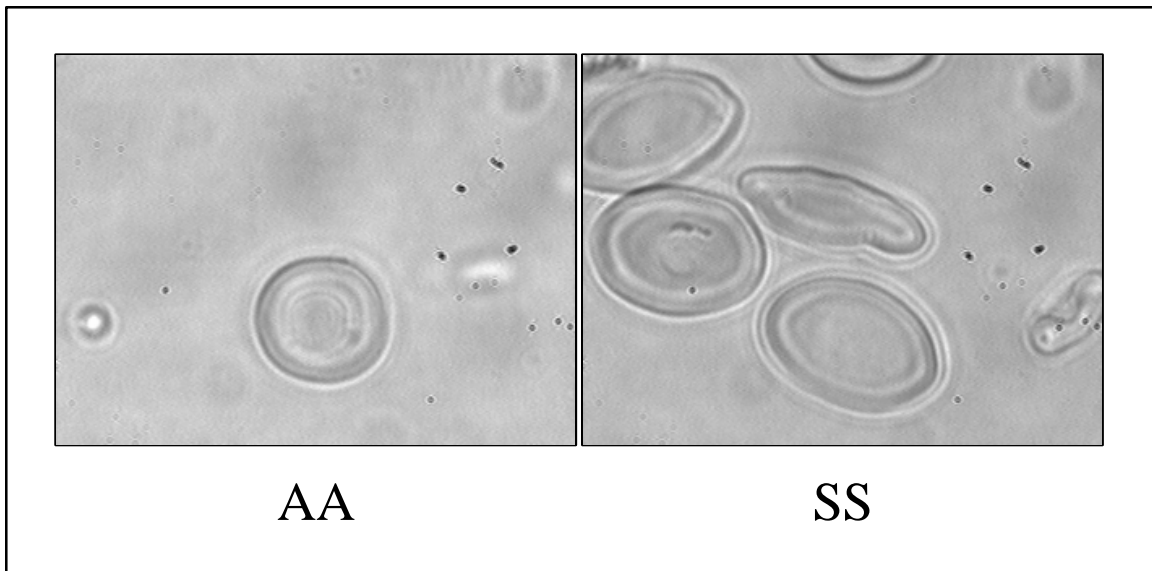


Figure 1.1: Typical Shapes for Normal (AA), and Sickle (SS) Red Blood Cells.

Finally, sickle hemoglobin has been found to be unstable. This unstability would be one the causes of some of the membrane abnormalities of sickle erythrocytes [Hebbel, 1991; Evans and Mohandas, 1987]. The real role of membrane abnormalities of sickle red blood cells is believed to add a "stochastic" influence on the potential of hemoglobin polymerization given at birth by the genetic code.

Sickle hemoglobin differs from normal hemoglobin, because the composition of the  $\beta$  chain provides an intermolecular contact that permits polymerization upon deoxygenation. Several studies have shown the effects of deoxygenation on blood rheology in sickle cell disease [Usami et al., 1975; Morris et al., 1993]. Other fellow researchers have worked on the determination of the polymer fraction (defined as the ratio of the amount of hemoglobin in polymer form, to the total amount of hemoglobin within the cell) and have highlighted the importance of this factor [Schechter and Noguchi, 1994; Hiruma et al., 1995]. So far, no correlation between sickle blood viscoelasticity and polymer fraction has been established.

Sickle cell anemia also causes a decrease of the oxygen tension due to a delayed passage of blood through capillaries, which can be explained by an increase in the bulk viscosity of the blood. At normal concentrations in oxygen, sickle cells do not show any abnormality in their microvascular flow. However, they exhibit higher internal cell viscosity, lower membrane elasticity, higher membrane viscosity mainly due to higher concentrations of hemoglobin [Chien et al., 1970]. At normal concentrations in oxygen, sickle cells show a slower microvascular flow. When fully oxygenated, sickle cells have a higher viscosity than normal cells. An increase in the amount of sickle hemoglobin polymer is noticed at low oxygen concentrations [Chien et al., 1970].

Oxygen is carried in blood in a dissolved form and is also chemically bound to hemoglobin [West, 1979]. Henry's law indicates that the amount of dissolved oxygen is linearly related to the partial pressure in oxygen. Otherwise, oxygen is chemically combined with



hemoglobin to give oxyhemoglobin ( $O_2 + Hb \leftrightarrow HbO_2$ ). The dissociation curve, shown in Fig. 1.2 shows the relationship between the partial pressure in oxygen ( $PO_2$ ) and the saturation in oxygen ( $SO_2$ ). The position of this curve and its gradient are both a function of a combination of factors (partial pressure in carbon dioxide ( $PCO_2$ ), pH, and temperature).

The effects of deoxygenation on blood rheology in sickle cell disease have been studied [Usami et al., 1975]. Usami and co-workers investigated the effects of deoxygenation by controlling the suspending medium, cell concentration (hematocrit at 45 %), shearing condition, temperature, gas tension and pH. A rotary-type tonometer was used for the control of gas tension.

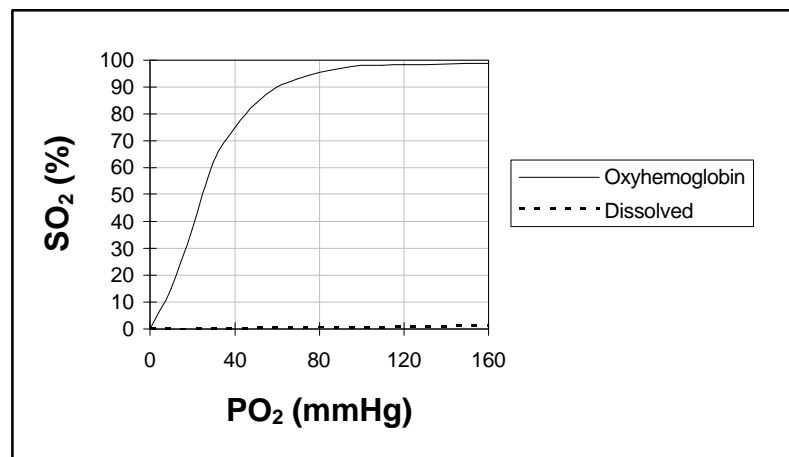


Figure 1.2: Dissociation Curve - Relationship between the Partial Pressure in Oxygen and the Saturation in Oxygen.

The  $CO_2$  concentration in the gas mixture was kept at 5.6 % in order to maintain the pH of the sample around 7.4. It was shown that the viscosity of suspensions of HbSS erythrocytes in plasma and in Buffer solution increased progressively when the  $PO_2$  was reduced below a

critical level of approximately 60 mmHg (equivalent to a saturation in oxygen of 80 %). No significant changes of viscosity with deoxygenation were found for HbAA erythrocytes (either in plasma or in Buffer solution).

The quantitative relationship between deoxygenation and rheological behavior of sickle cell suspensions and concentrated HbSS solutions was studied under steady shear (viscosity,  $\eta$ ) and oscillatory shear (complex viscosity, viscous and elastic components,  $\eta'$ ,  $\eta''$ ) by Chien et al., [1982]. The apparatus used was the same than Usami et al., [1975]. An increase in  $\eta$ ,  $\eta'$ ,  $\eta''$  for sickle cell suspensions and HbSS was found for a decrease in  $O_2$  saturation below 80-85 %. Apparently, as  $O_2$  saturation decreases, the viscoelastic properties of the sickle cell suspensions become dominated by that of the intracellular HbSS. Moreover, no changes were noticed for normal cell suspensions and HbAA solutions. Analysis of the data on suspensions of HbSS erythrocytes in plasma suggests that red blood cell aggregation decreases with deoxygenation and that both cell deformability and suspending media have to be considered in the analysis of rheological disturbances in sickle cell anemia.

Although the rheological behavior of sickle erythrocytes is highly dependent on oxygen tension ( $PO_2$ ) and temperature [Coffey, 1991], very little data exist regarding the effects of individual SS cells at body temperature. A system with  $PO_2$  and temperature control, using a micropipette aspiration was designed by Itoh et al. [1992]. This system was capable of monitoring  $PO_2$  at body temperature, and studying a single cell under microscopic observation. The micropipette technique is useful to study single cell deformability, including cell membrane

properties [Hochmuth et al., 1993]. The media with different  $PO_2$  was changed in a constant temperature chamber. As  $PO_2$  was decreased, the static rigidity and the dynamic rigidity showed no significant changes before sickling. But once sickled, morphologic alteration of the cell as well as an increase for the static and dynamic rigidities (10 to 1000 times) were observed.

The effects of varying hematocrit levels on sickle red blood cell rheology are well documented [Schmalzer et al., 1987]. Apparent viscosity of mixtures of washed normal (AA) and sickle (SS) red blood cells resuspended at varying hematocrit levels were measured by the means of a rotational viscometer. Viscosity results were expressed as a function of hematocrit levels, oxygen tension and shear rate. A positive linear relationship was found by Schmalzer and co-workers [1987] between viscosity and hematocrit for sickle cell suspensions. Substantial benefits were observed as the proportion of sickle cells was reduced (balanced with normal cells).

Another relevant factor in sickle cell anemia quantifying the ability of sickle erythrocytes to deform, is the filterability. The deformability of sickle cells can be studied using a tiny mesh filtration system. By air-equilibrating mixtures of sickle cell suspensions and sickle cells mixed with a known proportion of normal cells, the most influent factor in filterability happened to be the fraction of dense cells (defined as  $MCHC > 37$  g/dL) [Hasegawa et al., 1995]. The filtration of erythrocyte suspensions was impaired as the proportion of dense cells increased. This work had for aim of determining the optimal procedure for exchange therapy. It shows that reducing the proportions of non-dense and dense sickle cells circulating

is the key to improvement in the rheological characteristics of blood in SS patients regularly transfused. Filterability of AS and  $\beta^+$  Thalassemia red blood cells was expressed as a function of polymer fraction [Hiruma et al., 1995]. Sickle trait and sickle  $\beta^+$  Thalassemia were used because these cells present minimal membrane abnormalities and density heterogeneity. It was found that filterability has a linear relationship with polymer fraction, up to 30 % polymer fraction. This work confirmed that sickle hemoglobin polymerization is definitely the dominant factor in sickle cell anemia.

The biomechanical membrane changes of sickle erythrocytes are believed to occur after repeated polymerization-depolymerization processes [Hebbel, 1991]. Membrane abnormalities also occur due to the shrinkage of sickle cells (dense cells) [Dong et al., 1992]. These cells, which have a higher MCHC (>37 g/dL) exhibit a higher internal viscosity, which would explain the membrane abnormalities.

One important factor in sickle cell anemia is the cell density heterogeneity. Quantification of the erythrocytes density profile is well known [Rodgers et al., 1985]. Discontinuous Stractan density gradient technique was used to separate all the subpopulations of erythrocytes of close MCHC. It was found that sickle cells show a wider and broader distribution in its MCHC profile. This profile differs from normal cells by the presence of very light cells, and very dense cells, which are not found in a normal cell MCHC profile [Rodgers et al., 1985]. Dense cells are one of the most influent factor in the pathophysiology in sickle cell anemia as it has been already explained previously [Hasegawa et al., 1995] and [Hiruma et al., 1995].

Indeed, polymer fraction and impaired filterability are highly dependent on the proportions of dense sickle cells.

A method to measure the relationship between cell filtration and the formation of sickle hemoglobin polymer has been developed by Hiruma and co-workers [1995]. This system was used whether sickle cell morphology, independent of the polymer fraction was somehow related to the cell rheology. This work suggests that studies of sickle cell disease pathophysiology should consider the polymer fraction as a better parameter, rather than the cell morphology. It was found that the cell morphology was not strongly related to filtration and that on the other hand polymer fraction was.

Biochemical and Biophysical studies have led fellow researchers over the years to develop a thermodynamic analysis of the polymerization of sickle hemoglobin [Minton, 1977; Hofrichter, 1979; Gill et al., 1980, and Sunshine et al., 1982]. Based on this thermodynamic description, that predicts the behavior of polymer formation as a function of oxygen saturation, Noguchi and co-workers were able to generate the polymer fraction profiles as a function of oxygen saturation, as it will be explained in Chapter 2: Materials and methods. By using this new thermodynamic analysis, behavior of polymer in unfractionated blood can be predicted.

Rheological properties of sickle erythrocytes were measured as a function of  $PO_2$ , temperature, and also cell density using a micropipette setup by Mackie and co-workers [1990]. The mechanical properties measured were the shear modulus of membrane elasticity, the recovery time and the unfolding time constant. To relate their experimental data to the polymer fraction, partial pressure in oxygen, temperature and

density were measured. Then, the  $PO_2$ - $SO_2$  dissociation curve was used in order to read the corresponding values for the oxygen saturation. Bohr effects equations and polymer fraction versus oxygen saturation charts were used to express the mechanical properties as a function of polymer fraction.

The amount of polymerized sickle hemoglobin, can also be measured by using C/H magnetic double-resonance spectroscopy [Noguchi et al., 1979 and 1980]. This study shows that Nuclear Magnetic Resonance techniques can provide quantitative information about the ratio of intracellular hemoglobin in a polymer form to the total amount of hemoglobin within the cell. These techniques appear to provide accurate quantitative results and do not require separation of the sample into a fluid phase and a solid phase.

Although sickle cell anemia is genetically completely characterized, the sickling process is still not fully understood. Search for potential treatments for sickle cell anemia is still going on [Abraham et al., 1991; Johnson et al., 1994, and Reilly et al., 1993].

#### 1.4. Significance

In general, sickle cells are more rigid than normal cells due to less flexible membranes and higher intracellular viscosity. This is particularly true when red blood cells are deoxygenated. Sickle cells cause an increase in the bulk viscosity of blood. In severe cases the cells plug the smaller capillaries causing painful microvascular obstructions known as "sickle crisis". In such cases, the surrounding tissues are deprived of oxygen due to the decreased blood flow. The

purpose of this study is to simulate in vitro the effects of deoxygenation on sickle cells. By steadily decreasing the partial pressure in oxygen ( $PO_2$ ), blood is expected to reach a certain oxygen level at "equilibrium" after at most thirty minutes at the same  $PO_2$  (using a spin-cup tonometer, described in Chapter 2: Materials and methods). By recreating some of the physiological conditions and by measuring all the influent factors such as partial pressure in oxygen, saturation in oxygen, temperature, pH and osmolarity, rheological properties expressed in terms of viscosity can be consistently and accurately measured. All the red blood cell suspensions will be resuspended at 25 % hematocrit (either in autologous plasma or in Phosphate Buffer Solution), because sickle cell patients, who are anemic, usually exhibit a lower hematocrit than normal patients. To separate the effects of membrane abnormalities from that of the hemoglobin, both sickle trait (AS) and sickle cell (SS) blood will be used. Normal (AA) blood will be run as control, because we do not expect too much changes. To investigate the influence of plasma proteins, red blood cell suspensions will be resuspended at 25 % hematocrit in both their autologous plasma and Phosphate Buffer Solution. In order to isolate the effects of membrane abnormalities in sickle red blood cells, some experiments will be accomplished with hemoglobin solutions in their autologous plasma obtained by sonication as described in the Chapter 2: Materials and methods. Viscoelastic properties will be expressed as a function of partial pressure in oxygen and oxygen saturation. Eventually, the polymer fraction will be related to the steady-state viscosity for the first time. This relationship might tell us how the viscosity changes as a function of polymer

fraction, and if a relationship can be derived. The role of abnormal cell membrane as well as hemoglobin on the rheological behavior will then be discussed. This study might bring up some new insight. The newly designed ball microrheometer provides consistent and accurate viscosity measurements even for low viscosities (water viscosity can be measured), which is still unthinkable for most of the rheometers/viscometers discussed in paragraph 1.1. The ball microrheometer measures viscosities of red blood cell suspensions at 25 % hematocrit, which is from a clinical point of view, closer to the real physiological conditions. This new approach tending to relate polymer fraction to the viscoelastic properties will offer new elements, which, it is hoped, will lead in a long run to new clinical treatments.



CHAPTER 2  
MATERIALS AND METHODS

2.1. Instrumentation

2.1.1. Microrheometer Chamber

Viscoelastic measurements are performed in a modified magneto-acoustic ball microrheometer of Tran-Son-Tay et al. [1988]. A tiny stainless steel ball (Model 440-C, New England Miniature Ball CO., Connecticut) with diameters from 0.322 mm to 1.28 mm and density of 7.6675 g/ml is inserted in a cylindrical glass capillary tube (internal diameter of 1.61 mm and about 10-11 mm long) as it is shown in Fig. 2.1. The tube is held vertically within a Lexan<sup>TM</sup> water jacket with o-rings at each end to provide tight-seals. Because of the small sample size, the temperature of the sample fluid can be rapidly and accurately controlled with the help of a water bath (Model RTE 110, Nestlab, New Jersey). The sample volume required is about 20  $\mu$ l. The ball motion caused by a known force either constant or oscillating provides the measure of the steady-state viscosity and the complex viscosity of any sample respectively. Translucent as well as opaque samples can be studied.

An ultrasonic pulser/receiver (Model 5052 PR, Panametrics, Massachusetts) is used to track the motion of the ball. The pulser part of the instrument generates short, large amplitude pulses of controlled

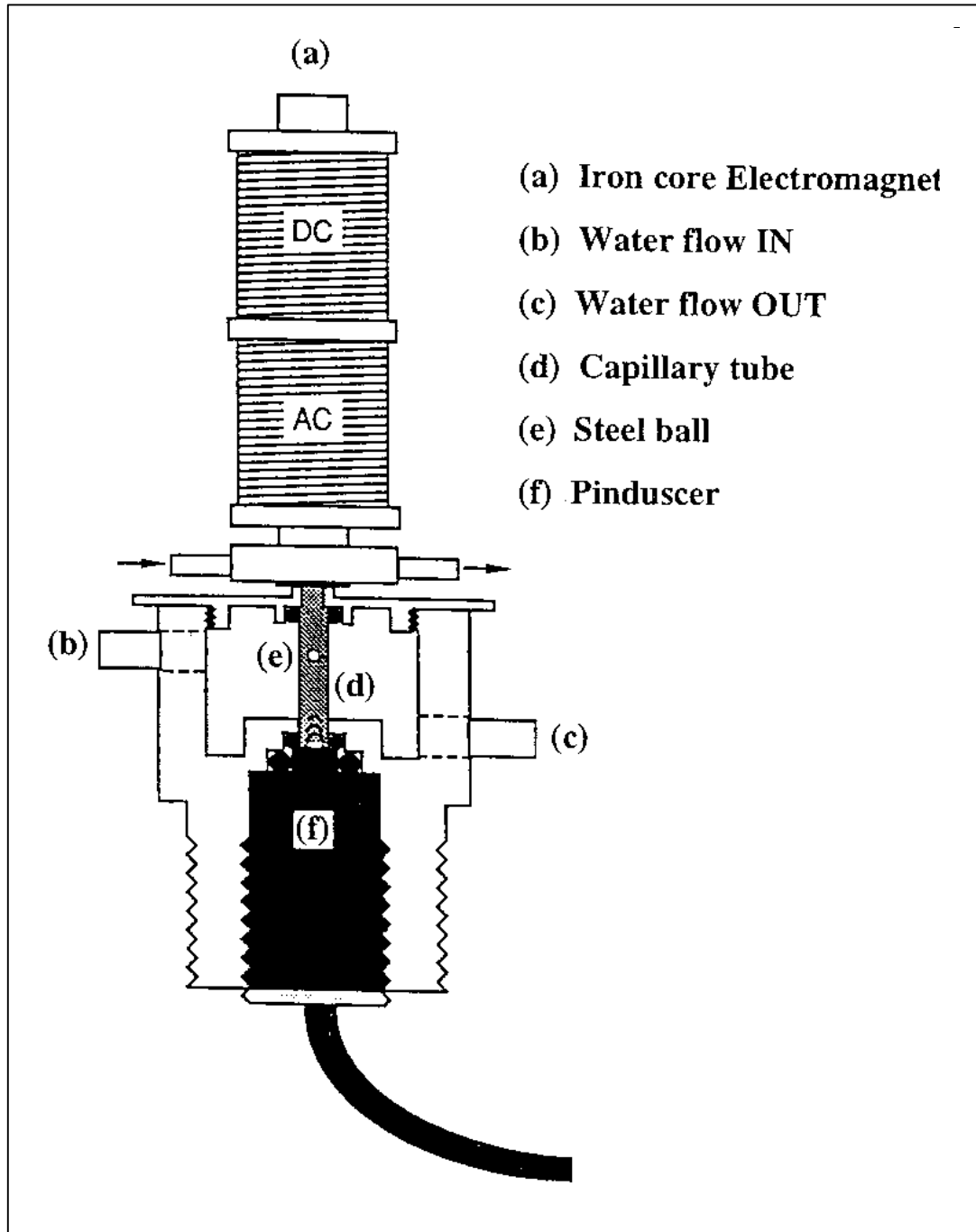


Figure 2.1: Microrheometer Schematic.

energy which when applied to an ultrasonic transducer are converted into short ultrasonic pulses. These ultrasonic pulses are received by the transducer (Model pinducer 15 MHz, Custom size  $\text{Ø}2$  mm, Valpey-Fisher, Massachusetts) after reflection from the top of the microrheometer chamber or the ball (when inserted). The receiver part amplifies and filters the voltage signal, produced by the reflected wave.

To drive the ball, an electromagnet is used as shown in Fig. 2.1. It consists of two copper wire sections wound about a soft iron core (sections: 36 gauges, 4000 turns each, iron core diameter: 1.3 cm for 5.5 cm in length). A three-way positioner (Newport Corporation, California) is used to precisely place the electromagnet above the chamber. A power supply (Model 1302, Global Specialties, New Jersey) provides a Direct Current (DC) component to the electromagnet for levitating and stabilizing the ball by counterbalancing gravitational forces. A sweep function generator (Model 3022, BK Precision, Illinois) followed by an amplifier (Model 6824 A, Hewlett Packard, Connecticut) generates an Alternating Current (AC) component strong enough to drive the electromagnet. In order to minimize any changes due to heating by current through the copper wire (section AC), a power resistor (100  $\Omega$ , 2 W) is placed in series with the electromagnet.

### 2.1.2. Time-to-Voltage Conversion

The newly redesigned microrheometer uses a Time-to-Voltage Conversion to track the motions of the ball. The Time-to-Voltage Conversion is a new concept in test and measurement instrumentation. It provides real time conversion of time interval measurements into voltage that can be displayed as a waveform on an oscilloscope. The vertical axis on the oscilloscope display represents the time interval measurement. The horizontal axis display represents the elapsed time. The oscilloscope waveform display gives a graphic representation of time-interval variations versus time. The Time-to-Voltage Converter (Model TVC 501, Tektronix, Florida; see Appendix A) measures:

1. Pulse width or period,
2. Delay between two independent signals.

The TVC 501 has three major functional blocks: the front panel, the processor board and the counter board as shown in Fig. 2.2. The front panel provides the user interface. The processor board provides general instrument control and generates triggers from the input signals.

The counter board performs Time-to-Voltage Conversions based on the duration of the input triggers coming from the processor board. The resulting output represents the Time-to-Voltage Conversion and is being processed as it is explained in the following schematic in Fig. 2.3.

The setup contains a Time-to-Voltage Converter, an ultrasonic pulser/receiver, two differential amplifiers, a pulse generator, a digitizing oscilloscope and a PC 486 DX 33 MHz.

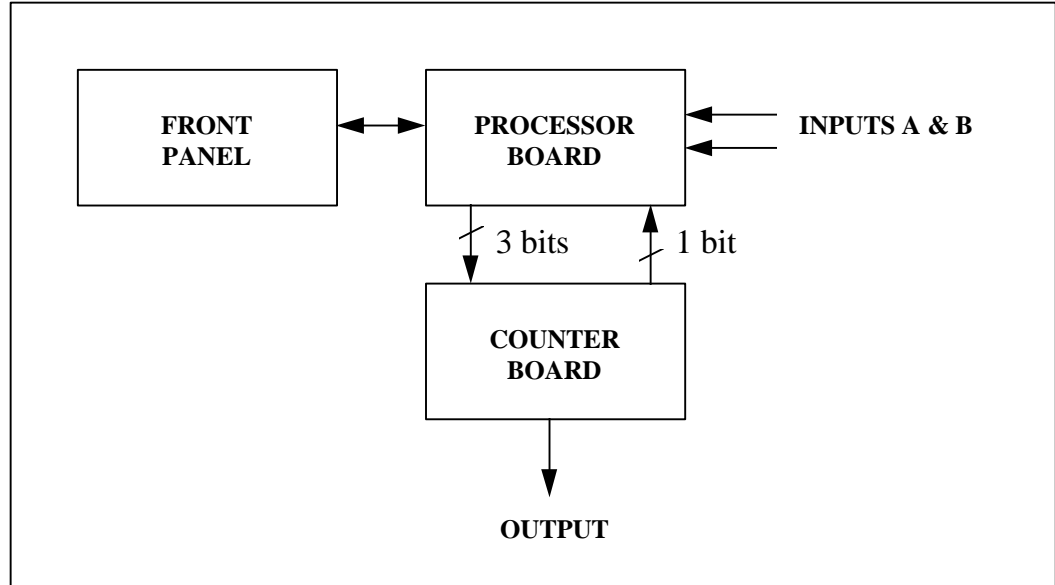
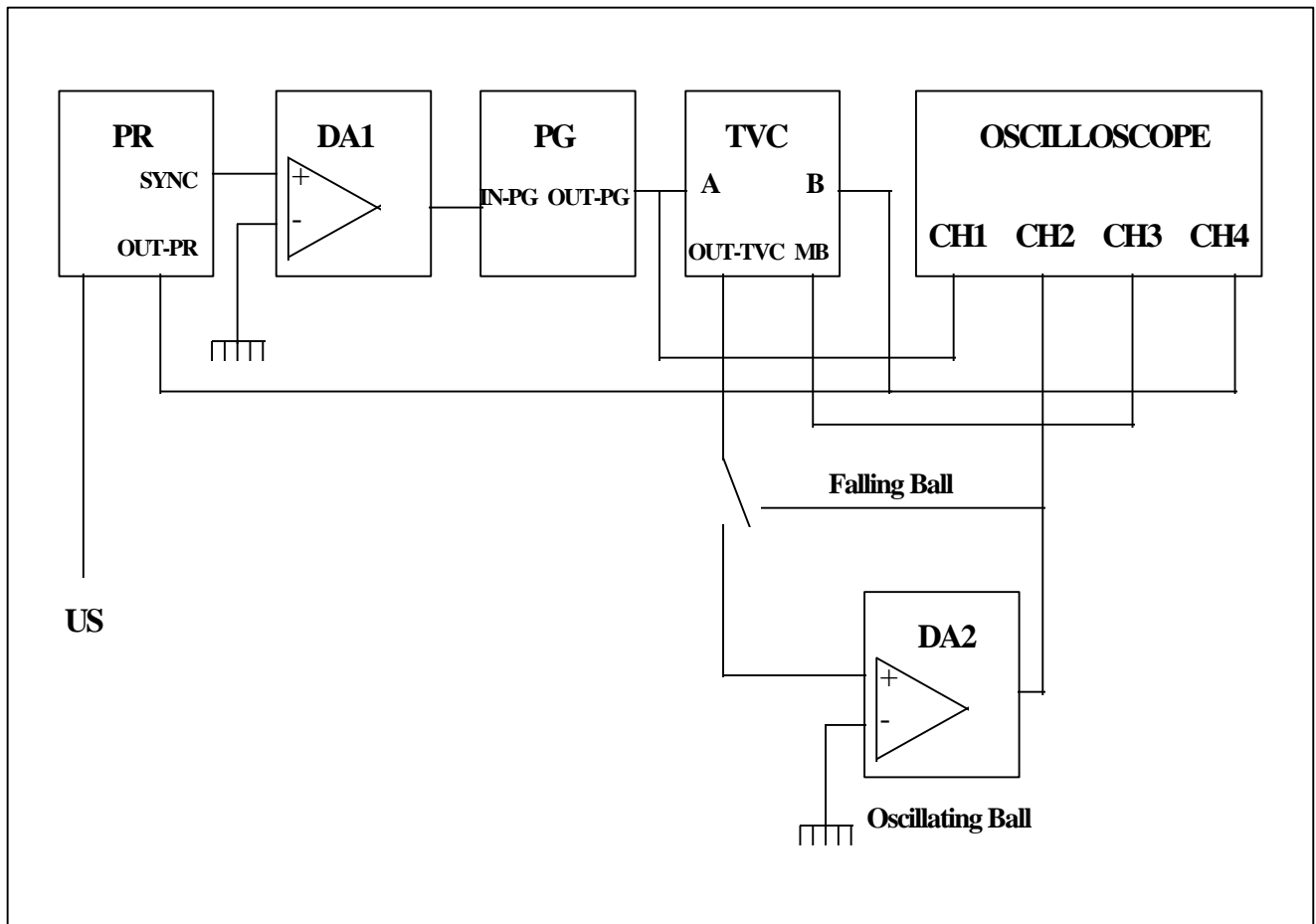


Figure 2.2: Simplified TVC Block Diagram.

The sound wave reflected back by the top of the chamber or by the ball coming from the ultrasonic pinducer (US) is being amplified filtered by the ultrasonic pulser/receiver and redirected through its output (OUT-PR) first to the digitizing oscilloscope channel 4 (CH4) for visualization and to the TVC input channel B. The synchronization signal (SYNC) provides a synchronizing pulse +2 V with an output impedance of 50  $\Omega$ . This signal will be used for triggering the pulse generator (IN-PG), which will generate the reference pulse used by the Time-to-Voltage Converter.

The synchronization signal must first go through a differential amplifier, where it will be modified to satisfy the pulse generator input restraints. The pulse generator output goes into the TVC input channel A and digitizing oscilloscope channel 1 (CH1). The TVC output monitor B (MB) is connected to channel 3 (CH3) and is being used as an indicator of



A: Channel A, Time-to-Voltage Converter (TVC 501)  
 B: Channel B, Time-to-Voltage Converter (TVC 501)  
 CH1 to CH4 : Channel 1 to Channel 4 oscilloscope (TDS 420)  
 DA1: Differential Amplifier (Model AM 502, Tektronix, Florida)  
 DA2: Analog Differential Amplifier  
 IN-PG: Input Trigger, Pulse Generator (PG 501)  
 MB: Monitor output B, Time-to-Voltage Converter (TVC 501)  
 Oscilloscope: Digitizing Oscilloscope (Model TDS 420, Tektronix)  
 OUT-PG: Positive pulse output, Pulse Generator (PG 501)  
 OUT-PR: Output Pulser/Receiver (PR 5052)  
 OUT-TVC: Output, Time-to-Voltage Converter (TVC 501)  
 PG: Pulse Generator (Model PG 501, Tektronix)  
 PR: Pulser/Receiver, (Model 5052 PR, Panametrics, Massachusetts)  
 SYNC: Synchro. signal, Pulser/Receiver (5052 PR)  
 TVC: Time-to-Voltage Converter (TVC 501, Tektronix)  
 US: Ultrasonic Transducer (Pinducer 15 MHz, Ø 2mm, Valpey-Fisher, Massachusetts)

Figure 2.3: Time-to-Voltage Converter Setup.

the state of the trigger based on the level and slope selected for the input channels. The TVC output (OUT-TVC) is the resulting voltage issued from the Time-to-Voltage Conversion and is connected to channel 2 (CH2) for visualization. Typical output for the digitizing oscilloscope channels (1, 3 and 4) are shown in Fig. 2.4.

$T_{tvc}$  is actually the time measured by the TVC technique which corresponds to the time interval between the top of the chamber or the bottom of the ball (point B) and the falling slope of the reference pulse (point A). The TVC provides real time measurement of  $T_{tvc}$  which allows accurate tracking of the ball motions.

### 2.1.3. Data Acquisition

The digitizing oscilloscope (Model TDS 420, 150 MHz, 100 Msamples/s, Tektronix, Florida) has a 24-pins GPIB connector on its rear panel. This connector has a D-type shell and conforms to IEEE standard 488-1-1987. By attaching an IEEE standard 488-1-1987 GPIB cable to the digitizing oscilloscope and to a GPIB plug-in-board (Model PCIIA, National Instruments, Texas), the device can be shared through a GPIB network. The digitizing oscilloscope GPIB parameters are first set to match the configuration of the bus (talk/listen modes). Then, the digitizing oscilloscope is driven through the GPIB interface using commands and queries. With the help of any DOS or Windows language, the oscilloscope can be commanded using the enhanced American Standard Code for Information Interchange (ASCII) character encoding. Commands and queries are encoded with the Backus-Naur-Form (BNF) notations and syntax diagrams (Programmer Manual, Part number 070-8709-06, Tektronix).

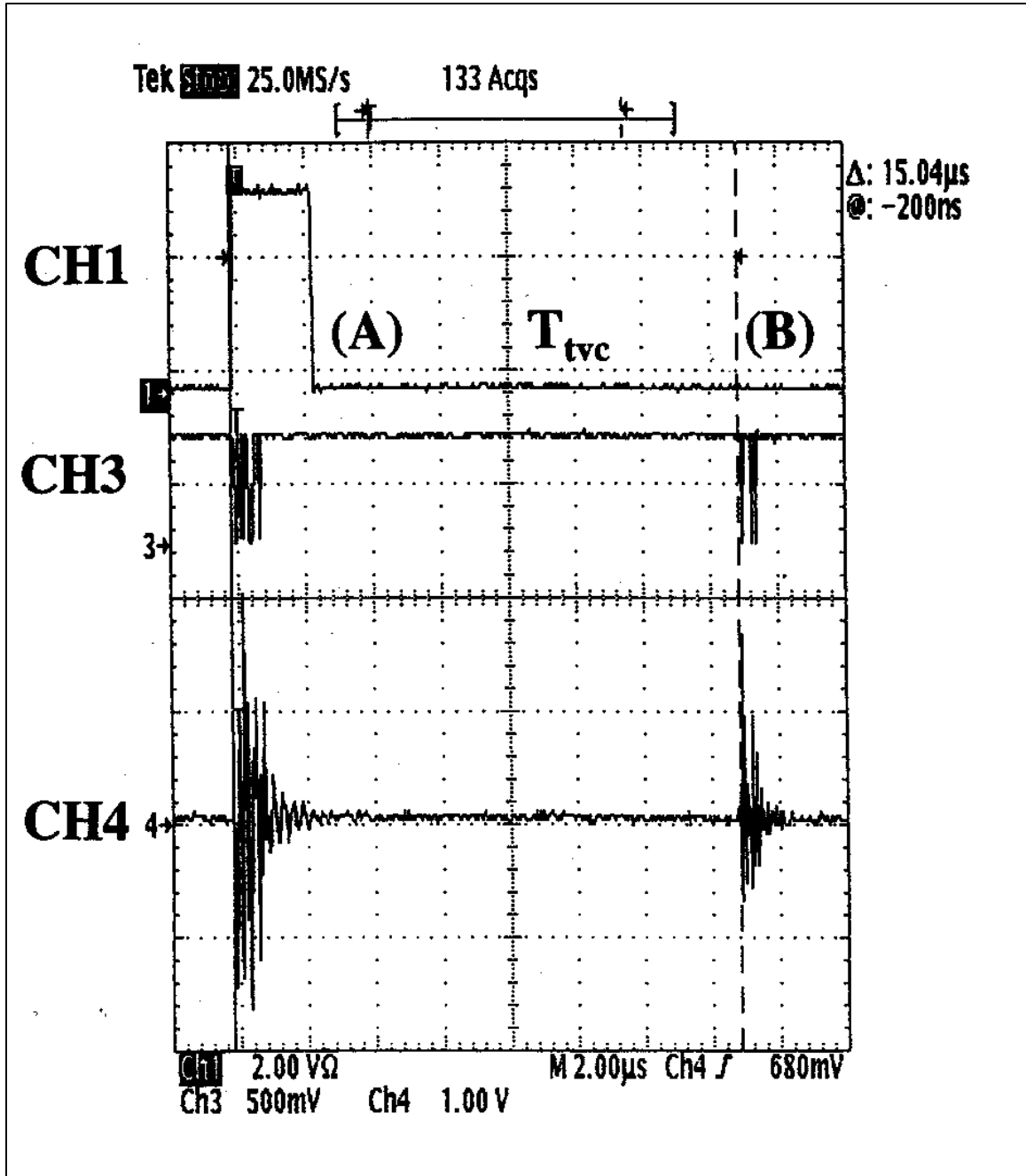


Figure 2.4: Typical TVC Measure.



In addition to the DOS language and the BNF syntax, the NI-488.2™ language (Part number 320282-01, National Instruments) is needed. This language is actually a low-level interface language in-between the DOS language and the ASCII-BNF character encoding standard. Commands modify instruments setting or tell the digitizing oscilloscope to perform a specific action. Queries cause the digitizing oscilloscope to return data and information about its status.

All these data transfers are ensured by a GPIB plug-in-board. It can be talker (give orders), listener (receive data) or controller. The role of the GPIB controller is comparable to the role of a computer CPU. It makes sure that all transfers are being processed within the shortest duration and without any risks of conflict with other CPU tasks.

A DOS language code has been written to take care of

1. Data acquisition,
2. Parameter's initialization,
3. Patient's information recording,
4. Consultation,
5. Proceedings of speed of sound, falling ball, oscillating ball experiments and GDM viscometry (Paragraphs 2.2., 2.3).

It has been written with the concern to reduce the interactions between the operator and the instruments and to offer the operator a convivial environment. Steady-state viscosity and complex viscosity are easily, quickly and accurately obtained (Appendix D: Program descriptive of data acquisition code).

#### 2.1.4. Controls of Partial Pressure in Oxygen and Oxygen Saturation

The aim of this study is to investigate the effects of deoxygenation on sickle cells. An entire new setup has been designed in this objective and includes the capabilities of measuring the partial pressure in oxygen and oxygen saturation. A spin-cup tonometer (Model IL 237, Instrumentation Laboratory, Massachusetts, lent by Dr. A.N. Schechter, MD, NIH, Maryland), three flowmeter units respectively for oxygen, nitrogen and carbon dioxide, a chemical microsensor and a co-oximeter are parts of this new setup as it is shown in Fig. 2.5.

The flowmeters (Model Accucal™, Gilmont, Illinois) are variable area flowmeters (rotameters). These meters consist of a spherical float moving vertically in a glass tube with a tapered inside diameter. As the flow through the tube increases, the float rises in the tube. A scale marked on the tube (along with calibration charts) is used to obtain accurate measurements of flow rate.

The co-oximeter (Model AVOXimeter 1000, Avox Systems, Texas; see Appendix B) quickly measures the oxyhemoglobin saturation, the total hemoglobin concentration, and the oxygen content in a sample of whole blood, partially hemolysed and hemoglobin solutions in a disposable cuvette. The AVOXimeter uses five wavelengths to obtain accurate measurements of the oxyhemoglobin saturation (%HbO<sub>2</sub>) although four different hemoglobin species (oxyhemoglobin, deoxyhemoglobin, methemoglobin, carboxyhemoglobin) are present in the sample. The value on the display for oxyhemoglobin saturation is defined as

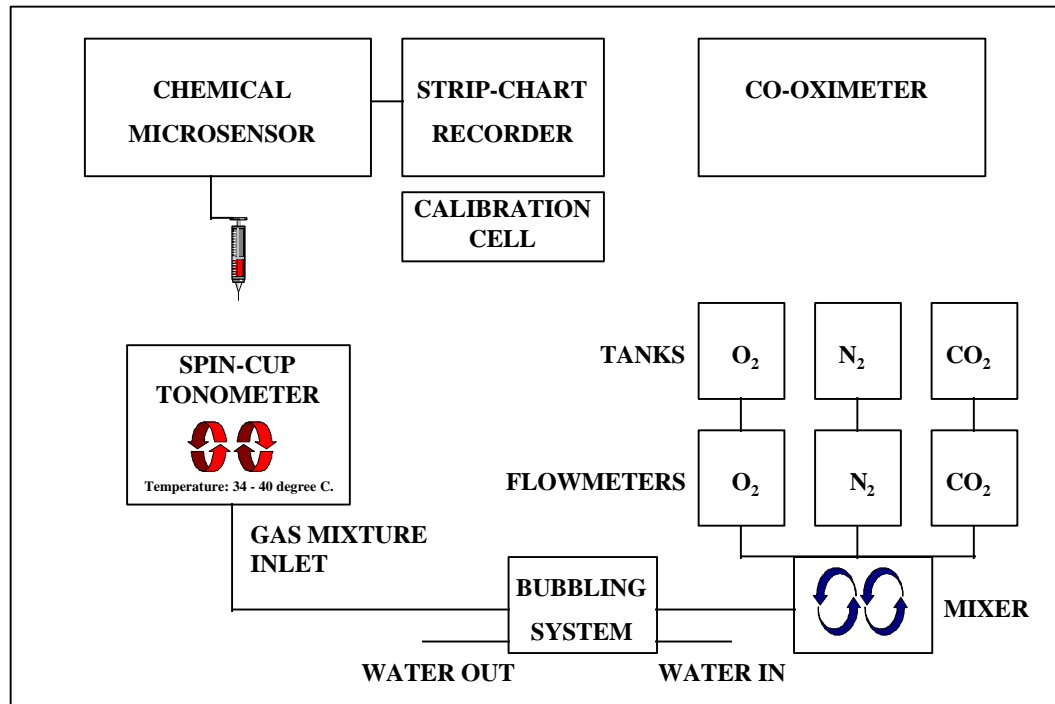


Figure 2.5: Controls of Partial Pressure in Oxygen and Oxygen Saturation.

$$\%HbO_2 = \frac{[HbO_2]}{[THb]}$$

$$[THb] = [HbO_2] + [Hb] + [MetHb] + [HbCO]$$

where

%HbO <sub>2</sub>	: Oxyhemoglobin saturation
[THb]	: Total hemoglobin concentration
[HbO <sub>2</sub> ]	: Oxyhemoglobin
[Hb]	: Deoxyhemoglobin
[MetHb]	: Methemoglobin
[HbCO]	: Carboxyhemoglobin

The chemical microsensor (Model 1231, Diamond General Development Corporation, Michigan; see Appendix C) is an instrument for amperometric measurements. For our application it will be utilized with a PO<sub>2</sub> polarographic sensing electrode (Model 757 oxygen needle electrode, Diamond General Development Corporation). This needle electrode has to be calibrated at its optimal polarization voltage (-0.7 V) for a constant temperature ( $\pm 0.2$  degree Celsius). The voltage-current relationship for a polarographic oxygen electrode is represented by the characteristic curve shown in Fig. 2.6. Under these conditions, the current flow through the electrode is directly proportional to the partial pressure in oxygen.

Because of the need to create a gas mixture, three flowmeters (Model Accucal<sup>TM</sup>, Gilmont) are required to measure the flow rates from each of the gas tanks. The chemical microsensor and the needle electrode must be calibrated at two different gas mixtures. Assuming current and percent oxygen are linear, only two gas concentrations are sufficient: zero O<sub>2</sub> (100 % N<sub>2</sub>) and ambient air (21 % O<sub>2</sub>). The temperature is kept constant (within  $\pm 0.2$  degree Celsius).

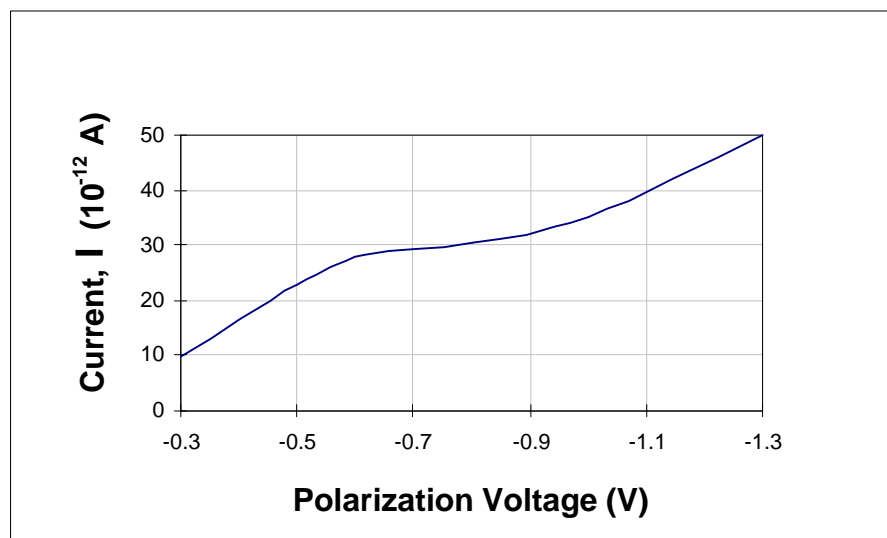


Figure 2.6: Characteristic Curve for a Polarographic Oxygen Electrode.

The prepared cells are then loaded into the spin-cup tonometer where a saturated mixture of  $O_2$ ,  $N_2$ ,  $CO_2$  gases awaits them. To prevent the cells from drying out, the gas mixture is saturated by bubbling it twice through water to ensure 100 % saturation humidity. After allowing thirty minutes for the cells to equilibrate at a given  $PO_2$ , the oxygen needle electrode is inserted in order to check the  $PO_2$  value. Then a 0.5 ml sample is withdrawn and used for the measure of saturation in oxygen,  $O_2$  content, total hemoglobin concentration and apparent viscosity.

## 2.2. Experiments at 37°C and Various $PO_2$

### 2.2.1. Speed of Sound

The speed with which sound waves are transmitted through a sample fluid is measured with the device by noting the time of flight for sound

pulses to travel from the transducer crystal to the top of the chamber and back. The chamber and transducer are designed such that the distance from the transducer to the top of the chamber is the same each time the instrument is assembled. It is essential that no air bubbles be introduced into the chamber with the sample, because air bubbles can dramatically increase sound attenuation and alter the speed of sound. A small syringe (Model 1 ml, Becton-Dickinson, Fisher Scientific, Pennsylvania) is used for loading gently the sample into the chamber.

The exact length of the chamber,  $H$ , is derived using distilled water at any temperature  $T_0$  for which the speed of sound,  $C_{H_2O}$ , is known [Del Grosso and Mader, 1972]. The time of flight (up and down),  $T_{H_2O}$ , is measured. Then the exact length can be expressed as follows:

$$H = 0.5 \times T_{H_2O} \times C_{H_2O}$$

Then the speed of sound of any sample fluid,  $C_{Sample}$ , can be derived by comparison of the time of flight through the fluid,  $T_{sample}$ , with  $T_{H_2O}$  and  $C_{H_2O}$  at the same temperature.

Hence,

$$2H = C_{Sample} \times T_{Sample}$$

$$C_{Sample} = \frac{2H}{T_{Sample}}$$

### 2.2.2. Steady-State Viscosity Measurement

The constant rate of fall of a given ball along the axis of the tube through the fluid provides the steady-state viscosity measurement

as found by Tran-Son-Tay et al. [1988]. For falling ball experiments the shear rate, although constant in time, is not constant in the gap between the surfaces of the ball and the tube wall. This remark is especially relevant for non-Newtonian fluids, which show a shear rate dependent viscosity. After the ball is dropped, the data acquisition program orders the data transfer from the oscilloscope to an ASCII file. The terminal velocity of the falling ball,  $V_t$ , is then determined from the ASCII file. The terminal velocity of the ball in the sample is simply equal to the slope of the curve (Distance,  $X$ , versus elapsed time) as it is shown in Fig. 2.7. In order to derive the terminal velocity from the data points acquired a Voltage-to-Time Conversion as well as a Time-to-Distance conversion are needed (see Appendix A).

Once the terminal velocity is known, the steady-state viscosity,  $\eta$ , is simply derived from the following relation [Tran-Son-Tay et al., 1988]:

$$h = \frac{2g R_b^2 (\rho_b - \rho)}{9K V_t}$$

where  $g$  is gravity ( $981.0 \text{ cm/s}^2$ ),  $R_b$  is the radius of the ball (0.065 cm),  $\rho_b$  is the density of the ball (7.6675 g/ml),  $\rho$  is the density of the fluid and  $K$  is the wall correction factor (the wall correction factor was determined by numerical simulation from the ratio of the ball diameter to the glass capillary tube diameter, equal to 0.8077.  $K$  was found to be 82.93).

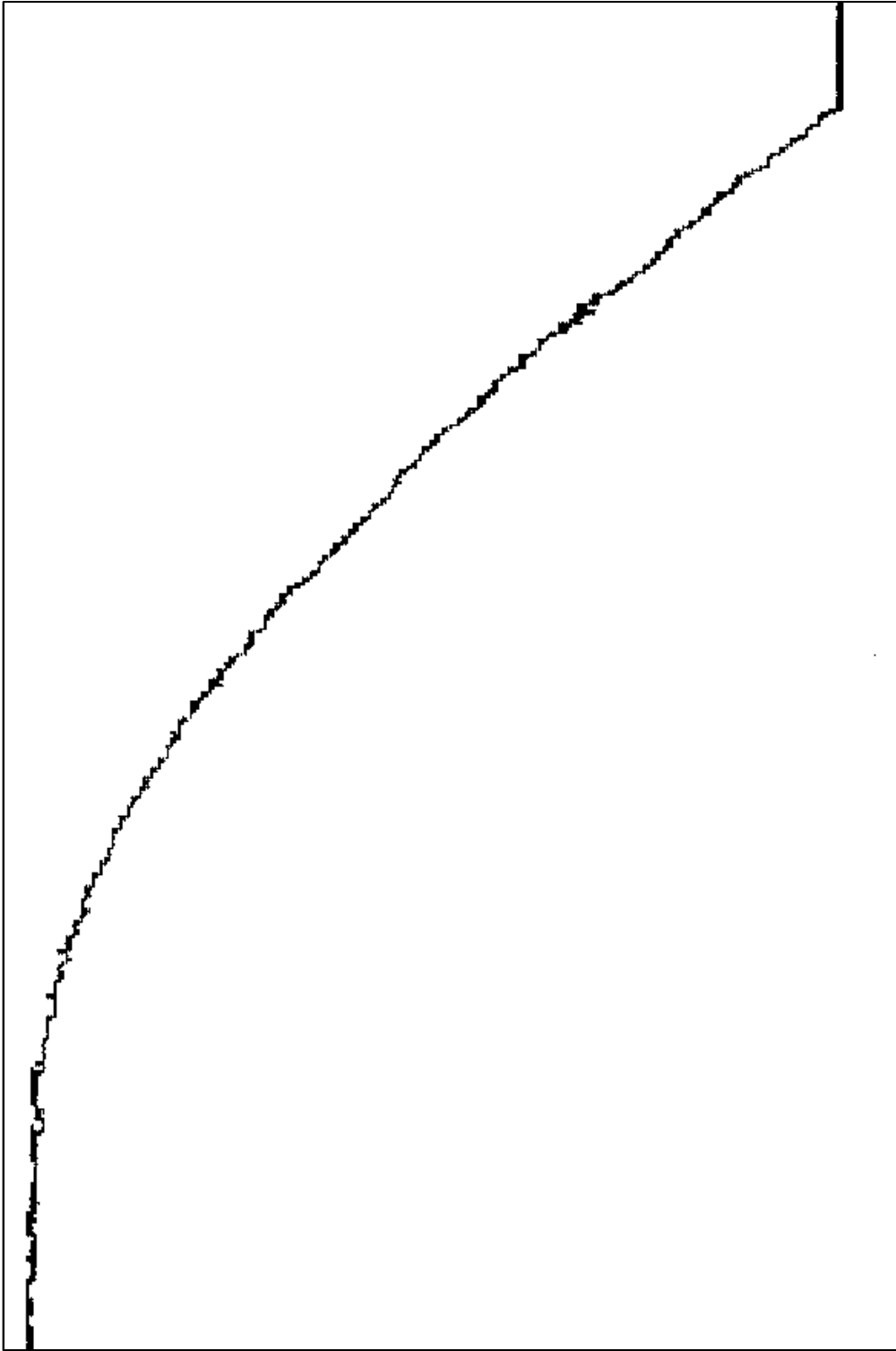


Figure 2.7: Typical Output for a Falling Ball Experiment.



### 2.3. Calibration

The calibration protocol consists in evaluating the performances of the whole setup in terms of precision, and consistency. The precision is defined in the present study as the intrinsic precision due to the electronic. The high sample rates for both the oscilloscope (150 MHz) and the Time-to-Voltage Converter (2.5 Msamples/s) provide accurate time measurements depending on the dynamic resolution of the TVC and the measured time interval. The precision corresponds to the total measurement error,  $E$  (in %), that the Time-to-Voltage Converter introduces during the conversion. It can be empirically expressed as follows:

$$E = \pm \left\{ 7 \times \frac{\text{Dynamic Resolution}}{\text{Time Measured}} + 0.25\% \right\}$$

For a measured time between 10 and 100  $\mu\text{s}$ , which is a typical time interval for falling ball experiments, the corresponding error,  $E$ , is:  $0.95\% > E > 0.32\%$ .

The consistency is related to the viscosity measurements. The new setup was calibrated by using distilled water and known viscosity silicone oils (Accumetric™, Kentucky) at 25°C. The speed of sound data in distilled water for temperatures between 5 and 37°C was compared to the data obtained by Del Grosso and Mader, [1972], as shown in Fig. 2.8. The densities were accurately measured with specific gravity bottles (Fisher Scientific). The oil viscosity was also determined using a Brookfield digital viscometer (Model RVTDCP, Brookfield, Massachusetts).

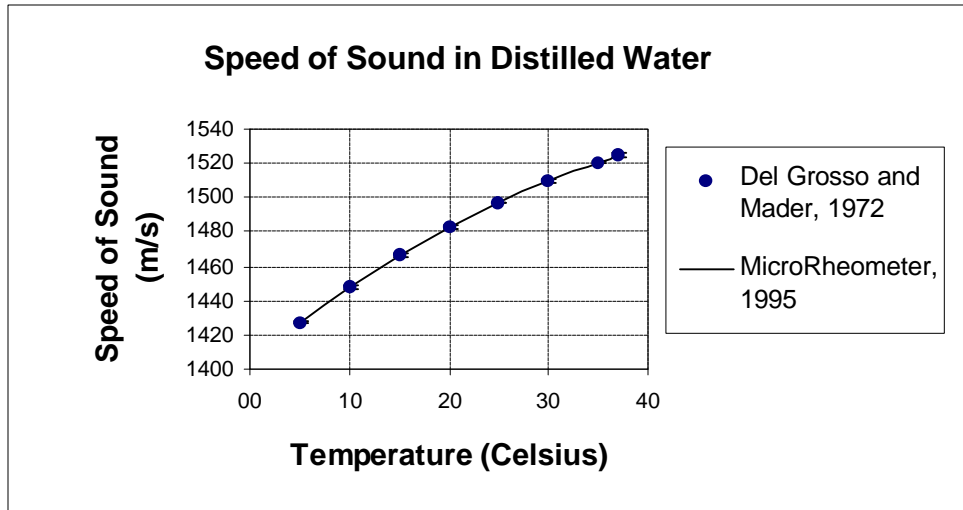


Figure 2.8: Speed of Sound in Distilled Water as a Function of Temperature.

The density of water was found to be 0.985 g/ml at room temperature and the densities of silicone oils were equal to 0.972 g/ml for 10 cSt (9.72 cP) and to 0.983 g/ml for 100 cSt (98.3 cP). The Brookfield digital viscometer, due to its range limitations (32 to 196600 cP) could not perform the measures for distilled water and silicone oil 10 cSt. The microrheometer found for the apparent viscosity of water at 25°C:  $0.98 \pm 0.03$  cP, which match the data found in the literature [Holman and Gajda, 1984]. Silicone oil 10 cSt was measured at  $9.58 \pm 0.15$  cP. Finally silicone oil 100 cSt viscosity was found to be  $95.09 \pm 2.59$  cP, to compare with the results of the Brookfield digital viscometer:  $94.99 \pm 0.97$  cP.

The microrheometer is used to measure the viscosity of red blood cell suspensions. Given as an example, Table 2.1 shows the apparent viscosity values for normal, and sickle red blood cell suspensions at 25

% and 45 % hematocrit, found by the microrheometer and in the literature.

Table 2.1: Viscosity Measurements of Normal, and Sickle Red Blood Cell Suspensions.

<b><u>Temperature: 37°C</u></b> <b><u>Normal Oxygenation</u></b> <b>Medium: Plasma</b>	<b><u>AA RBC</u></b> <b><u>Hct = 25 %</u></b> <b>(cP)</b>	<b><u>AA RBC</u></b> <b><u>Hct = 45 %</u></b> <b>(cP)</b>	<b><u>SS RBC</u></b> <b><u>Hct = 25 %</u></b> <b>(cP)</b>
<b>Literature</b> <b>[Ditenfass, 1985]</b>	X	5.44 ± 0.75 (30 men, 100 <sup>§</sup> Hct=46.8 ± 3.1 %)	X
<b>Microrheometer</b>	2.12 ± 0.057 (2 men, Hct=25 %)	4.08 ± 0.100 (4 men, Hct=45 %)	2.57 ± 0.106 (4 men, Hct=25 %)

#### 2.4. Blood Preparation

For these studies, blood from healthy donors, from donors with homozygous sickle cell disease and from sickle trait donors is collected by venipuncture into vacutainers using either Sodium Heparin as an anticoagulant. Blood is stored at 5°C and all measurements are made within 36 hours from withdrawal. To obtain the red blood cells, whole blood is centrifuged (Model Marathon 6K, Fisher Scientific) at 2000 g for 25 minutes after which the plasma and buffy coat are removed by aspiration and carefully stored. The red cells are then washed three times in isotonic Phosphate Buffered Saline solution (PBS) (Dulbecco's Phosphate Buffered Saline, D-PBS, 10 X). The pH of the PBS was previously adjusted to 7.4 (with 0.1 M HCl or 0.1 M NaOH) and its osmolarity was found to be 303 mosmol. The pH is measured with a digital pHmeter (Model 220, Corning, New York). Experiments are done at

25 % hematocrit to standardize the data. Hematocrit is measured by centrifugation of a 20  $\mu$ l sample at 13450 g for 3 minutes (Hematocrit tube, Cat-Number 1-000-7500-C, Fisher Scientific). By knowing the exact volume of packed cell suspensions (referred to in the text as suspensions of washed red cells, containing no plasma) and its hematocrit, one can derive the exact volume of either PBS or plasma and buffy coats to add (depending on if we want to resuspend these packed cell suspensions in their autologous plasma or in PBS). The suspensions are then equilibrated at ambient air for more than one hour, to ensure that all the samples start at a total oxygenation level (saturation in oxygen about 98.8 %).

#### 2.5. Hemoglobin Solution Preparation

Blood from healthy, homozygous sickle cell and sickle trait donors is also used to obtain hemoglobin solutions. The standard preparation of red blood cell suspensions resuspended at 25 % hematocrit either in their autologous plasma or in PBS remains the same as described previously in paragraph 2.4.

A sonicator (Model Virsonic 50, Fisher Scientific) is inserted into a 25 % hematocrit suspension of red blood cells. This sonicator supplies 23 kHz of high frequency electrical energy. This electrical energy is transformed into mechanical vibrations within the unit's converter by piezoelectric transducers. These ultrasonic vibrations are intensified and focused into the sample by an associated 1/8" diameter titanium microprobe, immersed with the sample solution. Extremely powerful shearing action is produced through the expansion and collapse

of millions of microscope vapor bubbles (cavities). This phenomenon known as cavitation, produces millions of miniature shock waves throughout the sample, causing the molecules in the liquid to become intensively agitated. Eventually, the cell membranes are broken, and so is obtained the hemoglobin.

The use of a glass cooling (Fisher Scientific) is needed in order to cool off the 2 ml sample to be sonicated at 5°C. The power range is set to 15 and the time of exposure is 30 s to 45 s. Within this interval, cell membranes are successfully broken without causing any aggregation. The hemoglobin solutions were systematically screened by checking a drop under microscopy (Model Axiovert 100, Zeiss, Germany) and see if it remains intact cells or not.

#### 2.6. Determination of Polymer Fraction

Several methods (as described in Chapter 1: Introduction and background) can be used to determine the extent to which the distribution in intracellular hemoglobin concentrations found in sickle erythrocytes affects the amount of intracellular polymerization of hemoglobin S.

Noguchi et al. [1983] and Noguchi [1984] developed a new numerical analysis to calculate the polymer fraction, as a function of oxygen saturation. The addition of the nonideal behavior of water in the solvent to the hemoglobin non-ideality in the thermodynamic description for hemoglobin S polymerization greatly improved the fit of the estimated prediction compared to the C NMR measurements [Noguchi et al., 1980].

By explicitly assuming that the intracellular hemoglobin and composition of sickle erythrocytes is known and uniform, Noguchi and co-workers [1980] can predict the behavior of polymer in unfractionated blood, based on the following new thermodynamic analysis.

The skeleton of this thermodynamic model was developed by Minton, [1977]. The nonideal behavior was added by Gill et al. [1980]. Assuming a homogenous cell population, the polymer fraction,  $f_p$ , can be derived as follows:

$$f_p = C_p (C_T - C_\sigma) / [C_\sigma (C_p - C_\sigma)]$$

where  $C_T = \text{MCHC}$ ,  $C_p =$  concentration of hemoglobin in the polymer phase (69 g/dL),  $C_\sigma =$  solubility of hemoglobin in the mixture expressed as a function of the oxygen saturation.

Using the density profile the calculated polymer fraction can be expressed as:

$$\begin{aligned} f_p &= \sum F_{ci} \times C_p [C_i - C_\sigma] / [C_\sigma (C_p - C_\sigma)] \\ &= \{C_p / [C_\sigma (C_p - C_\sigma)]\} \times \sum F_{ci} (C_i - C_\sigma) \end{aligned}$$

where  $F_{ci}$  is the fraction of cells with intracellular hemoglobin concentration  $C_i$ .

The whole theory has been summarized by Sunshine et al. [1982] and Noguchi et al. [1983]. An hemoglobin electrophoresis and a Complete Blood Count provide the proportions of hemoglobin (HbF, HbA, HbS) and the MCHC respectively. The solubility,  $C_\sigma$ , is calculated based on these parameters as explained in the theory. A code developed by C.T. Noguchi outputs the predicted polymer fraction,  $f_p$ , as a function of the saturation in oxygen.

CHAPTER 3  
THEORY

3.1. Speed of Sound

The microrheometer accurately measures the speed of sound,  $c$ , in any isotropic fluid. The speed of sound is defined as the speed at which sound waves propagate longitudinally through a fluid. It can be expressed for an adiabatic and reversible process, as follows:

$$c = \sqrt{\left(\frac{\mathcal{J}p}{\mathcal{J}r}\right)_r} \quad (3.1)$$

Defining the adiabatic compressibility,  $\beta$ , as

$$\mathbf{b} = \frac{1}{r} \left(\frac{\mathcal{J}r}{\mathcal{J}p}\right)_r \quad (3.2)$$

then, equation (3.1) may be expressed as a function of only two parameters, which are the adiabatic compressibility,  $\beta$ , and the density of the fluid,  $\rho$ , as shown by equation (3.3):

$$c = (\mathbf{r}\mathbf{b})^{-\frac{1}{2}} \quad (3.3)$$

Assuming that the fluid into question is a suspension of fine particles (meaning that the size of the particles is much smaller than the wavelength of the sound wave), then  $\beta$  and  $\rho$  can be respectively replaced by the relations (3.4) and (3.5) [Landau and Lifshitz, 1971]:

$$\mathbf{b} = (1-x)\mathbf{b}_{sf} + x\mathbf{b}_{sp} \quad (3.4)$$

$$\mathbf{r} = (1-x)\mathbf{r}_{sf} + x\mathbf{r}_{sp} \quad (3.5)$$

where  $x$  is the fractional volume of particles and where the subscripts  $sp$  and  $sf$  stand for Suspending Particle and Suspending Fluid, respectively. One condition for equations (3.4) and (3.5) to hold is that the particles be way smaller than the wavelength of the sound wave traveling through the suspension. With red blood cells, their diameter is about  $8 \mu\text{m}$ , which is roughly more than 10 times smaller than the wavelength of the sound wave ( $100 \mu\text{m}$ ). By combining equation (3.3) with equation (3.4), the adiabatic compressibility of a suspended particle,  $\beta_{sp}$ , may be expressed as shown by Tran-Son-Tay et al. [1989] by the following relation:

$$\mathbf{b}_{sp} = \frac{1}{x} \left[ x + \left[ \left( \frac{\mathbf{C}_{sf}^2}{\mathbf{c}^2} \right) \left( \frac{\mathbf{r}_{sf}}{\mathbf{r}} \right) - 1 \right] \right] \mathbf{C}_{sf}^2 \mathbf{r}_{sf} \quad (3.6)$$

This shows that if the characteristics of a suspension are known (density, hematocrit and speed of sound through the suspension) then the compressibility of individual red blood cells may be derived. The Mean Corpuscular Hemoglobin Concentration (MCHC) can be calculated from the compressibility values by using the linear fit that Shung et al. [1982] have found:

$$\text{MCHC} = 187.48 - 4.44 \times 10^{-12} \times \beta \quad (3.7)$$

where MCHC is in g/dL and  $\beta$  in  $\text{cm}^2/\text{dyne}$ .



### 3.2. Steady-State Viscosity

The steady-state viscosity, also known as apparent viscosity is the result of the falling ball experiment. The apparent viscosity of blood is not an intrinsic property of blood, but it is a property that depends on the data reduction procedure. The falling ball experiment is typically the case of a Stokes flow around a falling sphere. Stokes flow is described as a steady flow of an unbounded fluid around a ball, at low Reynolds number ( $Re \ll 1$ ). The drag force ( $F_{\text{Unbounded}}$ ) as well as the Archimedes's force ( $B_{\text{Unbounded}}$ ) are known to be the two forces that exert the fluid to resist to a falling object moving through the fluid as shown in Fig. 3.1.a.

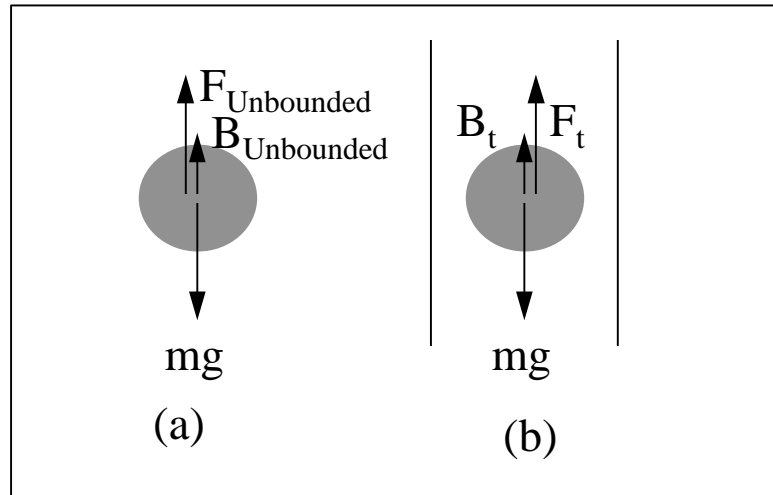


Figure 3.1: Falling Ball in:  
(a) Unbounded Fluid and (b) Cylindrical Tube.

Assuming that the fluid into question has a constant density,  $\rho$ , and a constant Newtonian viscosity,  $\eta$ , then the drag force can be expressed as it has been shown by Stokes [1851]:

$$F_{\infty} = 6\mu R_b h V_{\infty} \quad (3.8)$$

where  $R_b$  is the radius of the ball and  $V_{\infty}$  is the terminal velocity of the ball.  $F_{\infty}$ , known as the Stokes drag force, which is the drag force for an unbounded viscous fluid does not count any effects due to the presence of a container wall (Fig. 3.1.b). The wall correction factor,  $K$ , can be determined for various ball-to-tube diameter ratio,  $\lambda$ , as presented in Fig. 3.2.  $K$ , is defined as the ratio of  $F_t/F_{\infty}$ , where  $F_t$  is the total drag on the falling ball in a viscous fluid within a cylindrical tube. The ratio  $\lambda = R_b/R_t$  used in this study is 0.8077, and the appropriate wall correction factor,  $K$ , is 82.93.

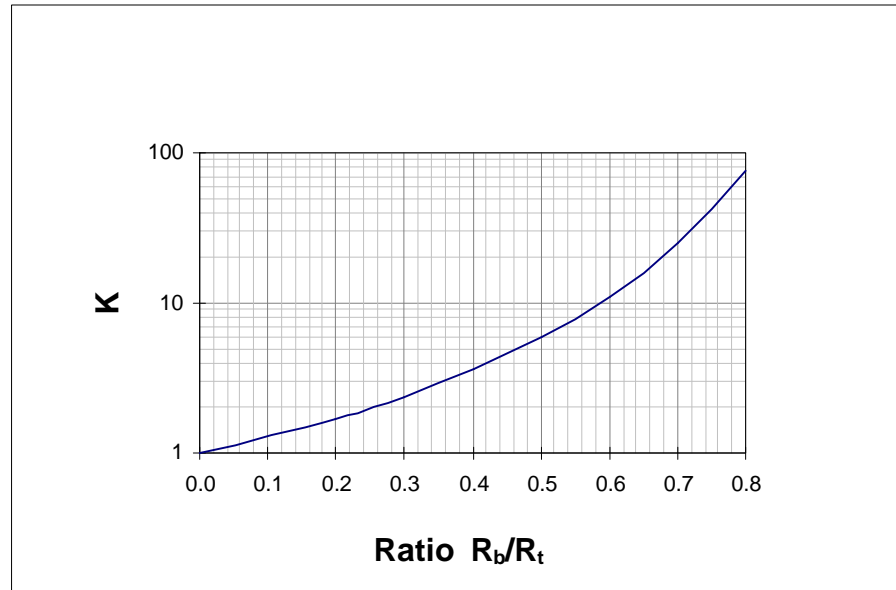


Figure 3.2: Wall Correction Factor,  $K$ , for a Rigid Sphere with Radius,  $R_b$ , within a Cylindrical Container with Radius,  $R_t$ , Moving Axially in a Purely Viscous Fluid.

The total drag  $F_t$  is expressed as follows:

$$F_t = 6\mu K R_b h V_t \quad (3.9)$$

where  $V_t$  is the terminal velocity of the ball falling axially through the tube.

The buoyant weight is defined as

$$\frac{4}{3}\rho R_b^3 g \mathbf{r} \quad (3.10)$$

where  $\rho$  is the density of the fluid. Equation (3.10) added to the total drag,  $F_t$ , must be equal to the weight of the ball:

$$\frac{4}{3}\rho_b R_b^3 g \mathbf{r}_b \quad (3.11)$$

where  $\rho_b$  is the density of the ball. By combining equations (3.9), (3.10) and (3.11), the steady-state viscosity,  $\eta$  (apparent viscosity), may be derived:

$$h = \frac{2g R_b^2}{9K V_t} (\mathbf{r}_b - \mathbf{r}) \quad (3.12)$$

By measuring the terminal velocity,  $V_t$ , of a falling ball in a fluid (with a known density,  $\rho$ ), then the steady-state viscosity of this fluid can be calculated.

CHAPTER 4  
RESULTS

4.1. Blood Analysis

A total of twelve individuals were studied: two normal, five sickle trait and five sickle cell donors. A two milliliters sample was systematically drawn and sent to the University of Florida, Shands Hospital, where an Hemoglobin Electrophoresis (HbE) and a Complete Blood Count (CBC) were done within six hours after the blood was drawn. Proportions of the different types of hemoglobin were determined from the Hemoglobin Electrophoresis, and the MCHC from the CBC. Results of the hemoglobin electrophoresis are presented in Table 4.1 and the Complete Blood Count results are shown in Table 4.2. Donors:

- 1 to 5, are sickle trait donors,
- 6 to 10, are sickle cell donors,
- 11 and 12 are normal donors.

Sickle cell anemia is one of the hemoglobinopathies, characterized by a type of hemoglobin with altered oxygen affinity, that causes anemia and other clinical consequences. Sickle cell individuals are expected to be anemic, which is confirmed by the CBC results (Table 4.2, see their hematocrit, Hct, and total hemoglobin concentration, [Hb]). Sickle cell donors clearly exhibit a lower hematocrit:  $26.3 \pm 5.8 \%$ , than normal donors:  $43 \pm 3.2 \%$ , as shown in Table 4.1. Sickle trait donors present a slightly lower hematocrit, than normal donors:  $37.6 \pm 2.8 \%$  (normal range: 33 and 49, males and females included).

Table 4.1: Hemoglobin Electrophoresis Results  
 (Numbers followed by "H" are High values, by "L" are Low values).

	PATIENT	HbA <sub>2</sub> /C (%)	HbS (%)	HbF (%)	HbA (%)	Remark	MCV (fL)	Hct (%)	Sex/Race
<b><u>AS</u></b>	PATIENT 1	1.00	34.90	0.30	63.80		83.80	39.40	F/B
	PATIENT 2	2.80	41.60	0.20	55.40		88.80	36.20	F/B
	PATIENT 3	2.70	34.10	0.00	63.10		80.50	41.50	M/B
	PATIENT 4	A2 present	40.00		58.00			34.50L	F/B
<b><u>SS</u></b>	PATIENT 5	2.20	39.30	0.10	58.40		84.60	36.20	F/B
	PATIENT 6	A2 present	84.00	14.00		Hydroxyurea	92.00	23.80L	F/B
	PATIENT 7	3.00	97.00			B-Thalassemia	71.00L	20.00L	M/B
	PATIENT 8	A2 present	98.00				91.00	27.90	F/B
	PATIENT 9	A2 present	73.00	26.00		Hydroxyurea	101.00H	24.40L	F/B
	PATIENT 10	A2 present	72.00	0.00	0.00	B-Thalassemia	69.00L	35.30	M/B
<b><u>AA</u></b>	PATIENT 11	1.20	0.00	0.00	98.80		89.10	45.20	M/W
	PATIENT 12	1.00			99.00		84.30	40.70	M/W

Table 4.2: Complete Blood Count Results  
 (Numbers followed by "H" are High values, by "L" are Low values).

	PATIENT	RBC ( $10^6/\mu\text{L}$ )	[Hb] (g/dL)	Hct (%)	MCV (fL)	MCH (pg)	MCHC (g/dL)	Platelet ( $1000/\text{cu}/\text{mm}$ )
<b><u>AS</u></b>	PATIENT 1	4.70	13.10	39.40	83.80	27.90	33.30	
	PATIENT 2	4.07	12.10	36.20	88.80	29.80	33.50	
	PATIENT 3	5.15	13.90	41.50	80.50	27.00	33.50	
	PATIENT 4	4.68	11.50L	34.50L	74.00L	24.60L	33.30	213.00
	PATIENT 5	4.28	12.00	36.20	84.60	28.10	33.20	
<b><u>SS</u></b>	PATIENT 6	2.59L	8.10L	23.80L	92.00	31.30	34.10	552.00H
	PATIENT 7	2.80L	6.60L	20.00L	71.00L	23.50L	32.90	591.00H
	PATIENT 8	3.08	9.10L	27.90	91.00	29.50	32.50	299.00
	PATIENT 9	2.42L	8.20L	24.40L	101.00H	34.00	33.80	516.00H
	PATIENT 10	5.09	11.50L	35.30	69.00L	22.60L	32.60	266.00
<b><u>AA</u></b>	PATIENT 11	5.08	15.40	45.20	89.10	30.20	34.00	
	PATIENT 12	4.82	14.10	40.70	84.30	29.30	34.70	

As a consequence, the total hemoglobin concentration for sickle cell individuals is only :  $8.7 \pm 1.8$  g/dL, as opposed to  $14.8 \pm 0.9$  g/dL for normal donors and  $12.5 \pm 1.0$  g/dL for sickle trait donors.

Individuals 6 and 9 are treated with Hydroxyurea, which is a drug that reduces the intracellular sickle hemoglobin concentration and increases fetal hemoglobin (Table 4.3). Sickle cell donors exhibit a clear disorder in their hemoglobin electrophoresis results. Only sickle hemoglobin and fetal hemoglobin were significantly present with:  $84.8 \pm 12.5$  % sickle hemoglobin and  $8.0 \pm 11.7$  % fetal hemoglobin.

Donors 7 and 9 are individuals with sickle  $\beta$  Thalassemia. Sickle homozygous  $\beta$  Thalassemia is a sickling disorder, that results from the bound between the sickle trait and  $\beta$  Thalassemia trait genes. This disease leads to no or severely reduced amount of normal hemoglobin. Fetal and  $A_2$  hemoglobins are usually found in larger proportions (Donor 7 shows 3 %  $A_2$  hemoglobin and no fetal hemoglobin; donor 9 presents 26 % fetal hemoglobin and only traces of  $A_2$ ; HbF and HbA<sub>2</sub> are two other types of normal hemoglobins). Table 4.3 summarizes the results of the hemoglobin electrophoresis and the CBC. Normal donors show values of normal hemoglobin close to 100 % as expected. On the contrary, sickle trait individuals, present  $38.0 \pm 3.3$  % of sickle hemoglobin and  $59.7 \pm 3.6$  % of normal hemoglobin. Almost no fetal hemoglobin was detected, less than 0.1 %.

Data presented in Table 4.3 are used to generate the polymer fraction profiles, given in Fig. 4.1. The determination of the polymer fraction is based on a thermodynamic analysis, that has been summarized in Chapter 2: Materials and methods. The polymer fraction profiles were generated by Dr. Noguchi and co-workers (NIDDK, NIH, Bethesda,

Maryland), using a code that expresses the polymer fraction in terms of the oxygen saturation. This program takes as inputs the respective proportions (in %) of normal hemoglobin, fetal hemoglobin, sickle hemoglobin (hemoglobins A<sub>2</sub> and C are fold with sickle hemoglobin), and finally the Mean Corpuscular Hemoglobin Concentration (MCHC in g/dL).

The four upper curves, donors 6 to 10 are the polymer fraction profiles for sickle cell individuals. The maximum polymer fraction formed is roughly 60 % at total theoretical deoxygenation of 0 % saturation in oxygen. There is polymerization of sickle hemoglobin for saturation in oxygen below 80 % for donors 6, 7 and 8, and below 70 % for donor 9. Polymer fraction curves for donors 6 and 9 (treated on Hydroxyurea) are beneath the profiles for donors 7 and 8. As expected, polymer fraction values for AS donors are much lower than for SS individuals. The five lower curves represent the polymer fraction profiles for the sickle trait donors 1 to 5. The maximum polymer fraction formed is approximately 30 % at total deoxygenation. Polymer starts forming for a saturation in oxygen below 50-55 %. It is essential to point the fact out that 50 % oxygen saturation is where the PO<sub>2</sub>-SO<sub>2</sub> dissociation curve is the steepest (see Chapter 1: Introduction and Background).



<b>PATIENT</b>	<b>HbA</b> (%)	<b>HbF</b> (%)	<b>HbS</b> (%)	<b>HbA<sub>2</sub>C</b> (%)	<b>MCHC</b> (g/dl)
<b><u>AS</u></b>	63.8	0.3	34.9	1.0	33.3
	55.4	0.2	41.6	2.8	33.5
	63.1	0.0	34.1	2.7	33.5
	58.0	0.0	40.0	Present	33.3
	58.4	0.1	39.3	2.2	33.2
<b><u>SS</u></b>	0.0	14.0	84.0	Present	34.1
	0.0	0.0	97.0	3.0	32.9
	0.0	0.0	98.0	Present	32.5
	0.0	26.0	73.0	Present	33.8
	26.0	0.0	72.0	Present	32.6
<b><u>AA</u></b>	98.8	0.0	0.0	1.2	34.0
	99.0	0.0	0.0	1.0	34.7

Table 4.3: Hemoglobin Electrophoresis and MCHC Summary.

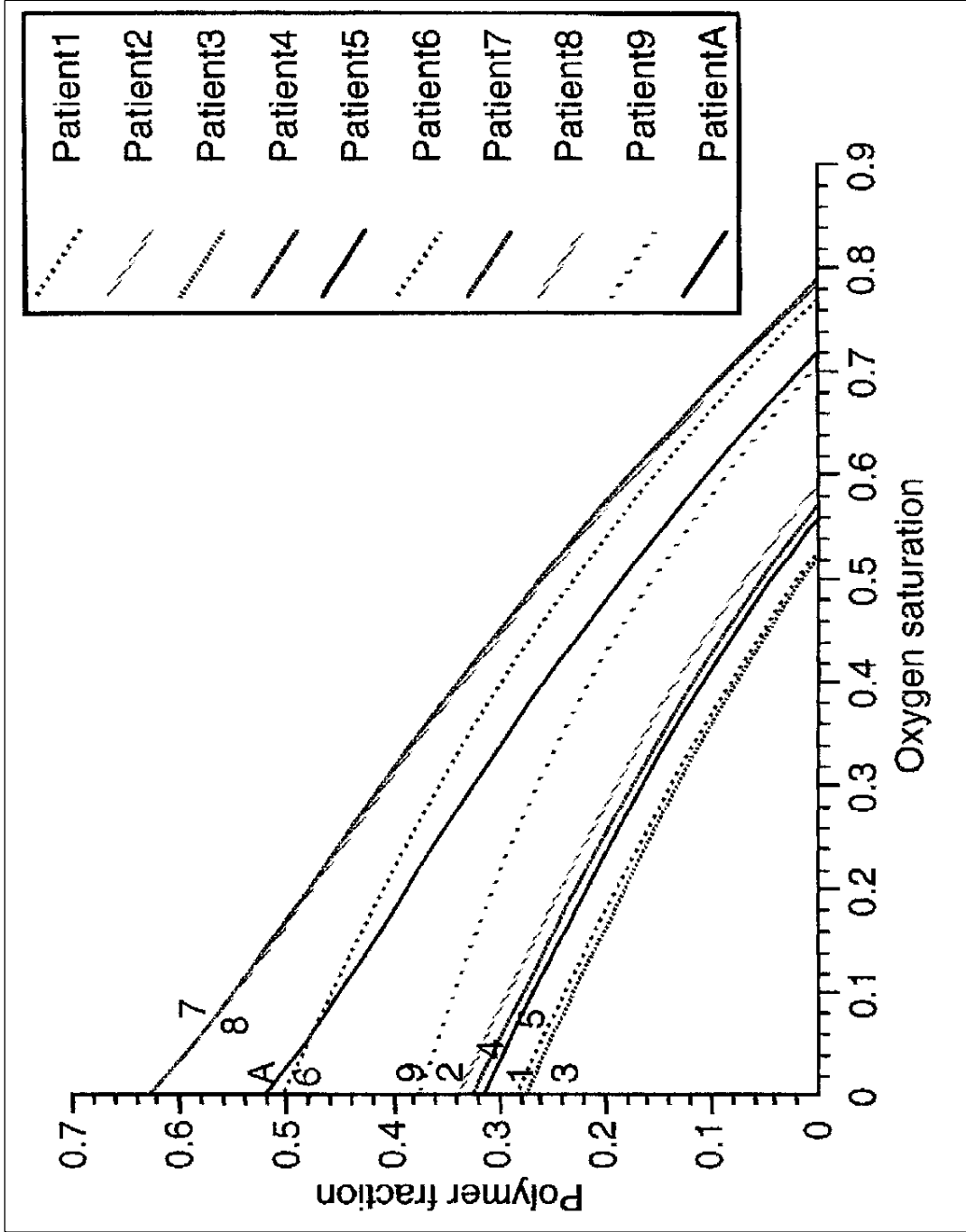


Figure 4.1: Polymer Fraction Profiles: donors 1 to 5 (AS) and donors 6 to 10 (SS).

#### 4.2. Red Blood Cell Suspensions in Plasma

Apparent viscosity ( $\eta$ ) for AA, AS, and SS red blood cell suspensions in plasma, as a function of  $PO_2$  and  $SO_2$  respectively, are given in Figs. 4.2 and 4.3. The same scale was used for all the plots presented in this chapter for easier comparison. Normal donors do not show any changes in their viscosity, as  $PO_2$  (Fig. 4.2.a) and  $SO_2$  (Fig. 4.3.a) decrease; a constant linear relationship is observed. On the other hand, sickle trait donors have a slight increase in their viscosity, as  $PO_2$  and  $SO_2$  decrease (Figs. 4.2.b and 4.3.b). Partial pressure in oxygen below 20 mmHg, equivalent to a saturation in oxygen of 30 %, seems to be the trigger level under which viscosity starts increasing. A statistical analysis showed that the best curve fit for the viscosity curves expressed in terms of  $PO_2$  (Fig. 4.2.b) and  $SO_2$  (Fig. 4.3.b) were logarithmic and linear respectively. The correlation coefficients for the  $PO_2$  curve were 0.67 (logarithmic), and 0.65 (linear). For the  $SO_2$  curve, the correlation coefficient was 0.76 (linear), against 0.69 (logarithmic). Eventually, sickle cell donors have a more pronounced increase in their apparent viscosity, for  $PO_2$  below 60 mmHg, or 70 % saturation in oxygen. The same statistical approach led to believe that a logarithmic fit is in this case, the most appropriate: 0.76 ( $PO_2$  curve, Fig. 4.2.c), and 0.79 ( $SO_2$  curve, Fig. 4.3.c).

Viscosity values as a function of polymer fraction are shown in Fig. 4.4. For normal donors, there is no polymer formation (Fig. 4.4.a). Sickle trait and sickle cell individuals data are presented in Figs. 4.4.b and 4.4.c respectively. Their trends will be discussed in Chapter 5: Discussion.

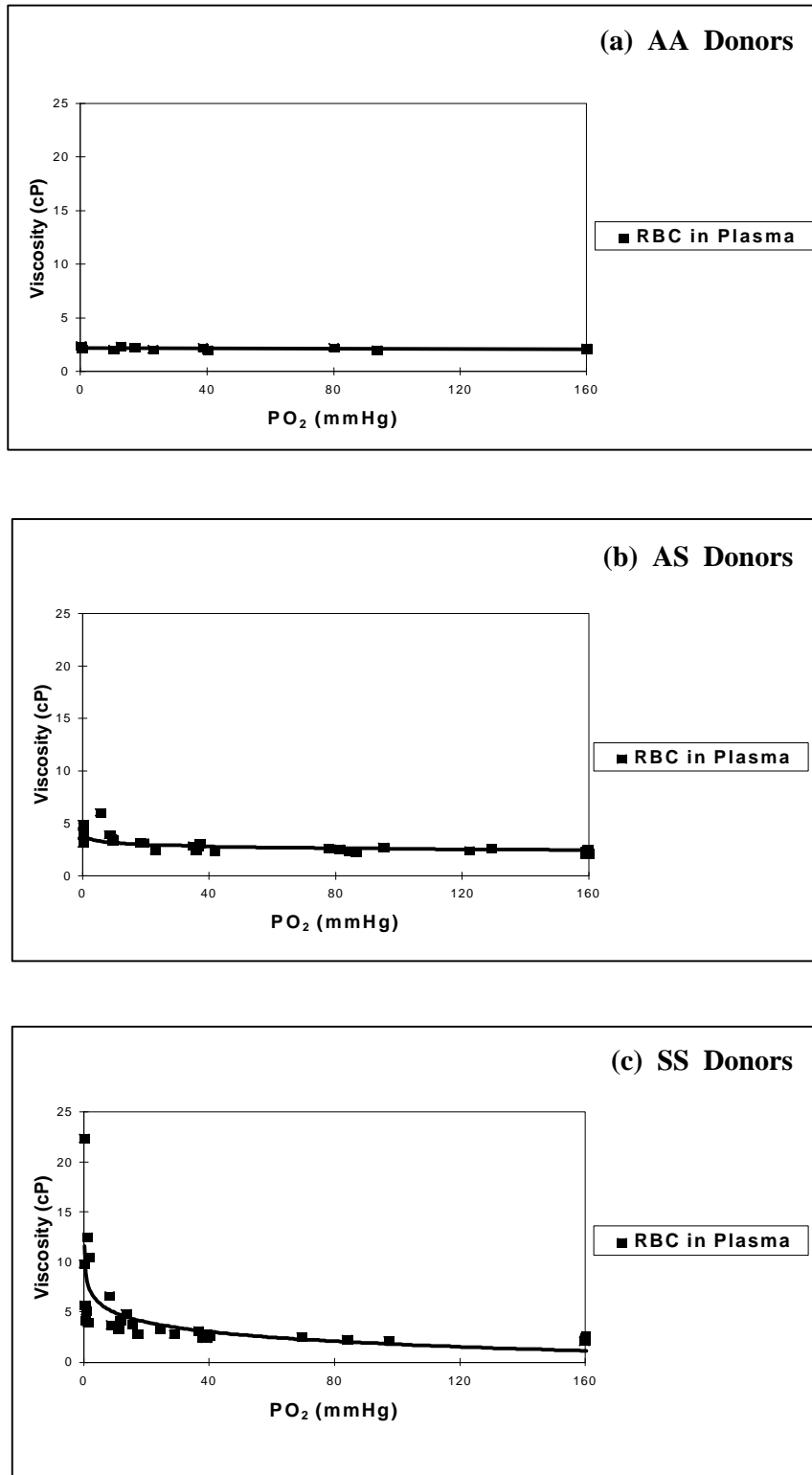


Figure 4.2: Apparent Viscosity vs. PO<sub>2</sub>:  
(a) AA donors, (b) AS donors, and (c) SS donors.

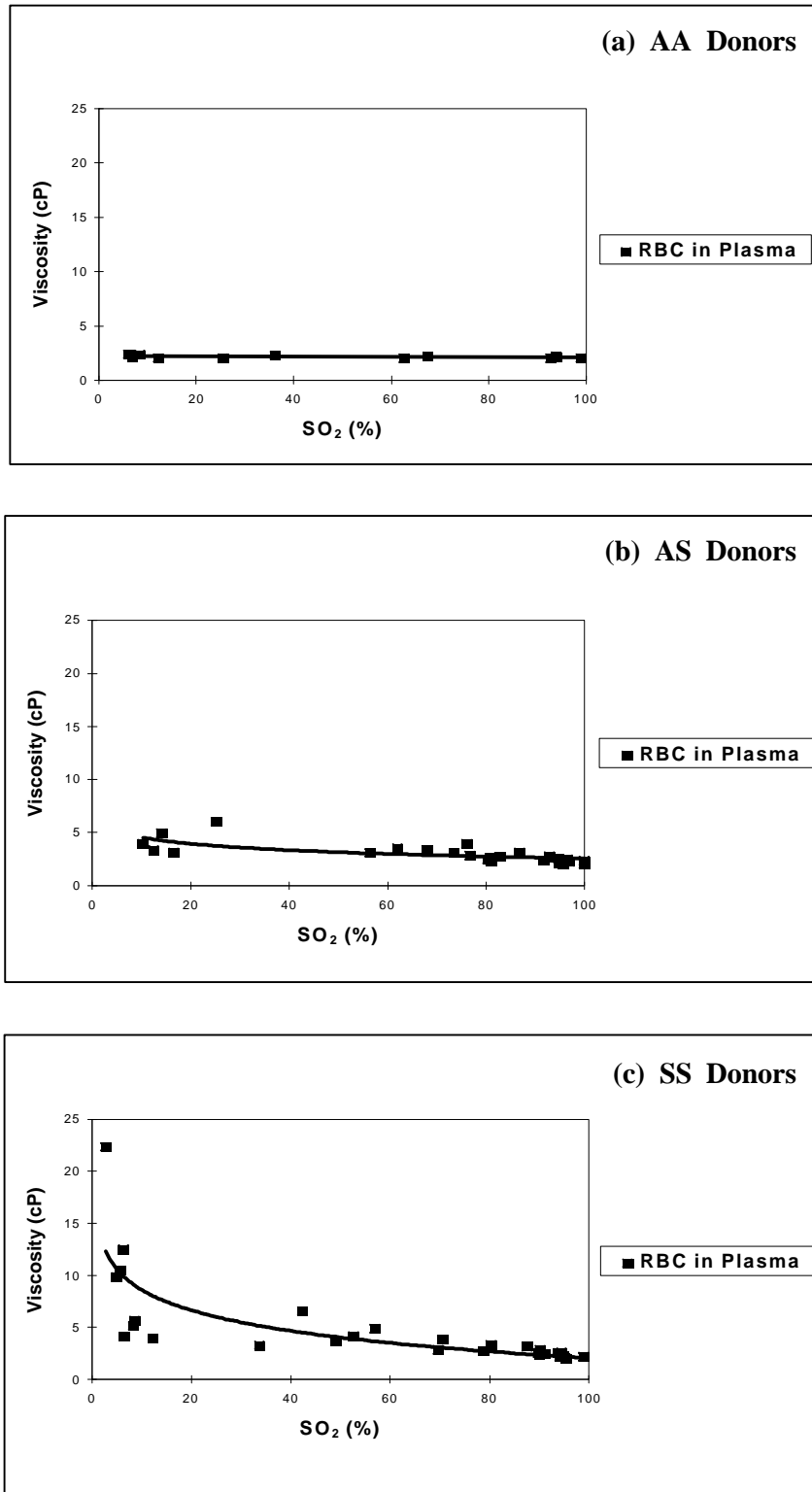


Figure 4.3: Apparent Viscosity vs.  $SO_2$ :  
(a) AA donors, (b) AS donors, and (c) SS donors.

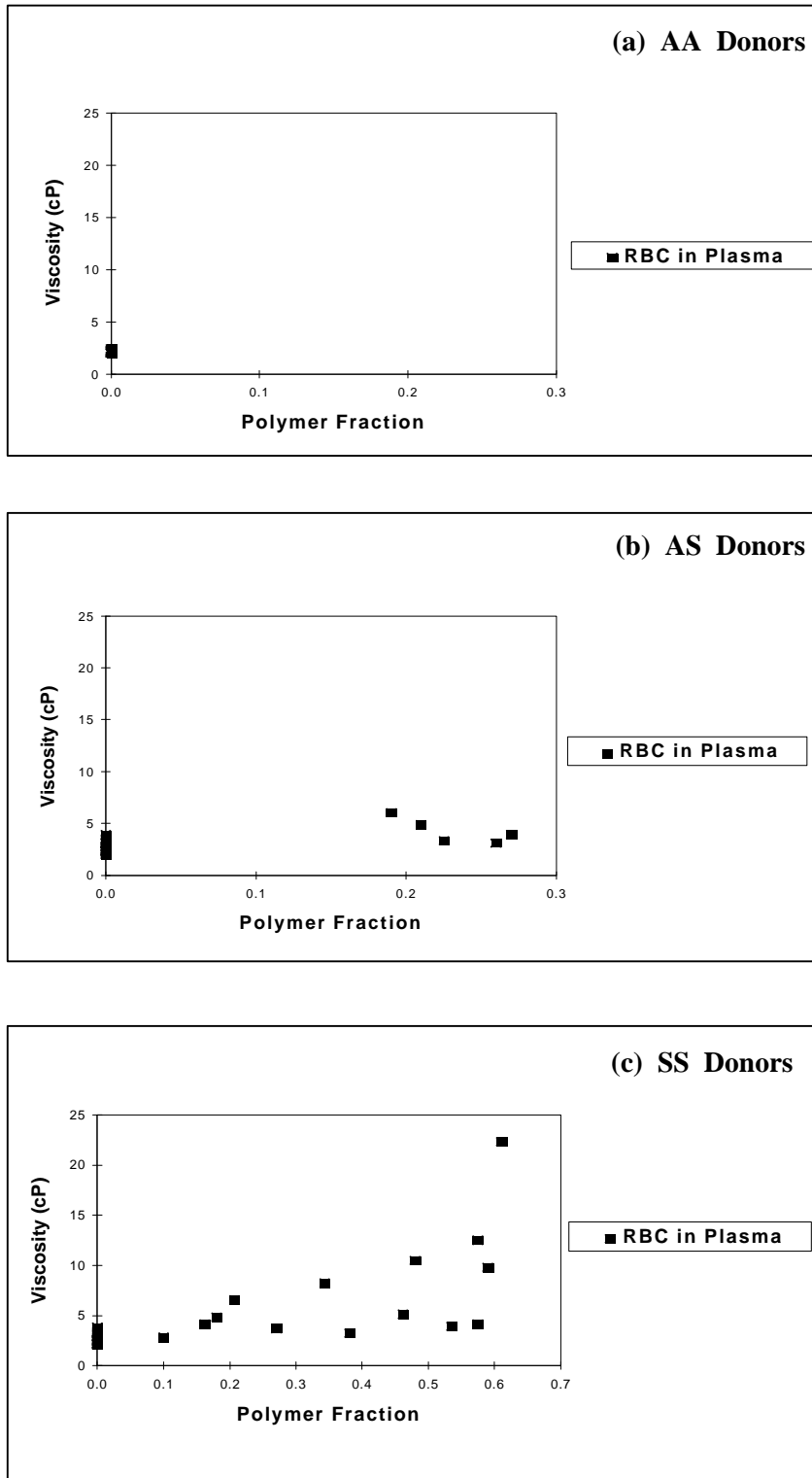


Figure 4.4: Apparent Viscosity vs. Polymer Fraction:  
 (a) AA donors, (b) AS donors, and (c) SS donors.

#### 4.3. Red Blood Cell Suspensions in Phosphate Buffer Solution

Figures 4.5, and 4.6 show the values of the apparent viscosity as a function of  $PO_2$  and  $SO_2$  respectively. Normal donors exhibit a flat linear relationship between viscosity values and  $PO_2$  (Fig. 4.5.a) and also  $SO_2$  (Fig. 4.6.a). Sickle trait individuals appear to exhibit the same trend (Fig. 4.5.b). However, the best curve fit was found to be logarithmic with a correlation factor of 0.71 (to compare with the linear regression: 0.56), suggesting that there is a non negligible increase at very low oxygen levels (below 20 mmHg). On the contrary, a linear relationship over the full range is found between  $\eta$  and  $SO_2$  (Fig. 4.6.b). Sickle cell donors once again show an increase in viscosity for  $PO_2$  below 60 mmHg (Fig. 4.5.c), steeper than for sickle trait donors. The best curve fit happened to be logarithmic rather than linear (0.74, against 0.53). This remark is also suitable for the viscosity plot expressed as a function of  $SO_2$  (Fig. 4.6.c) for which an increase in viscosity is again observed at saturation in oxygen below 70 %.

Curves of viscosity expressed as a function of polymer fraction are shown in Fig. 4.7. No polymer is formed inside RBC's from normal donors as expected (Fig. 4.7.a). A linear relationship is seen between viscosity and polymer fraction up to 30 % for sickle trait donors (Fig. 4.7.b). The relationship between apparent viscosity and polymer fraction for sickle cell individuals is shown in Fig. 4.7.c. The difference in amplitude in viscosity between plasma and PBS suspensions, suggesting a potential effect of plasma proteins will be addressed in Chapter 5.

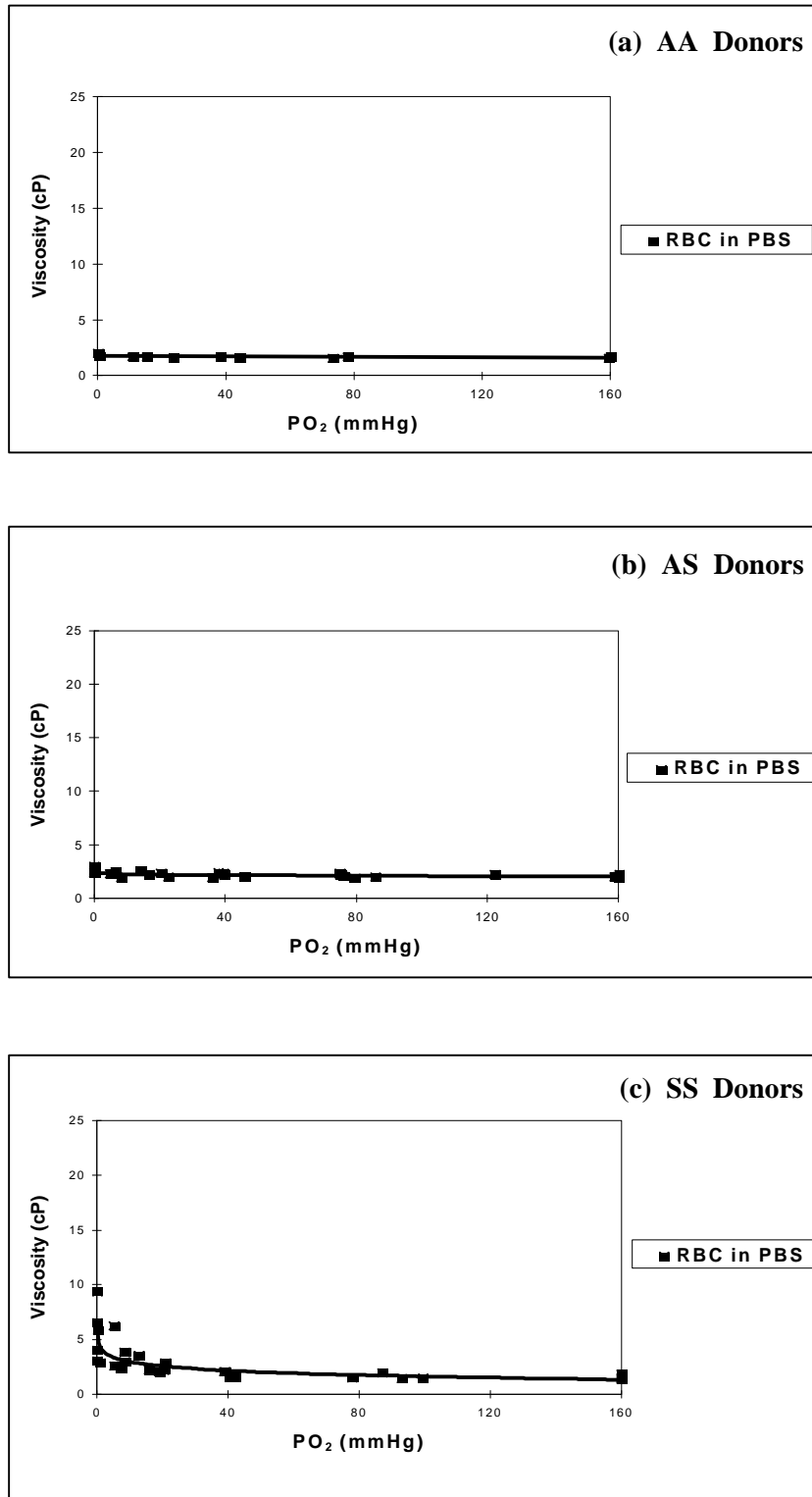


Figure 4.5: Apparent Viscosity vs. PO<sub>2</sub>:  
(a) AA donors, (b) AS donors, and (c) SS donors.



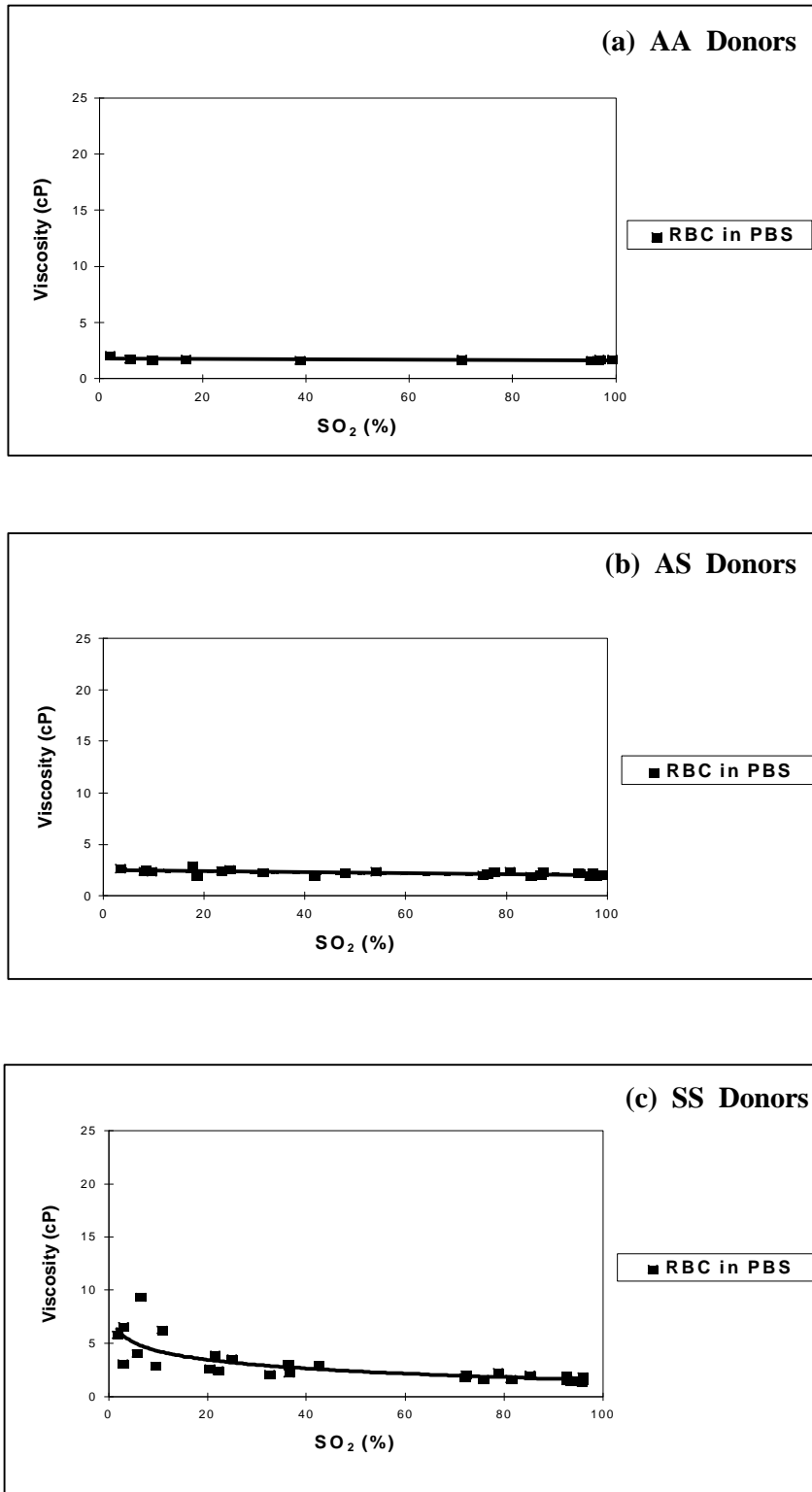


Figure 4.6: Apparent Viscosity vs.  $\text{SO}_2$ :  
(a) AA donors, (b) AS donors, and (c) SS donors.

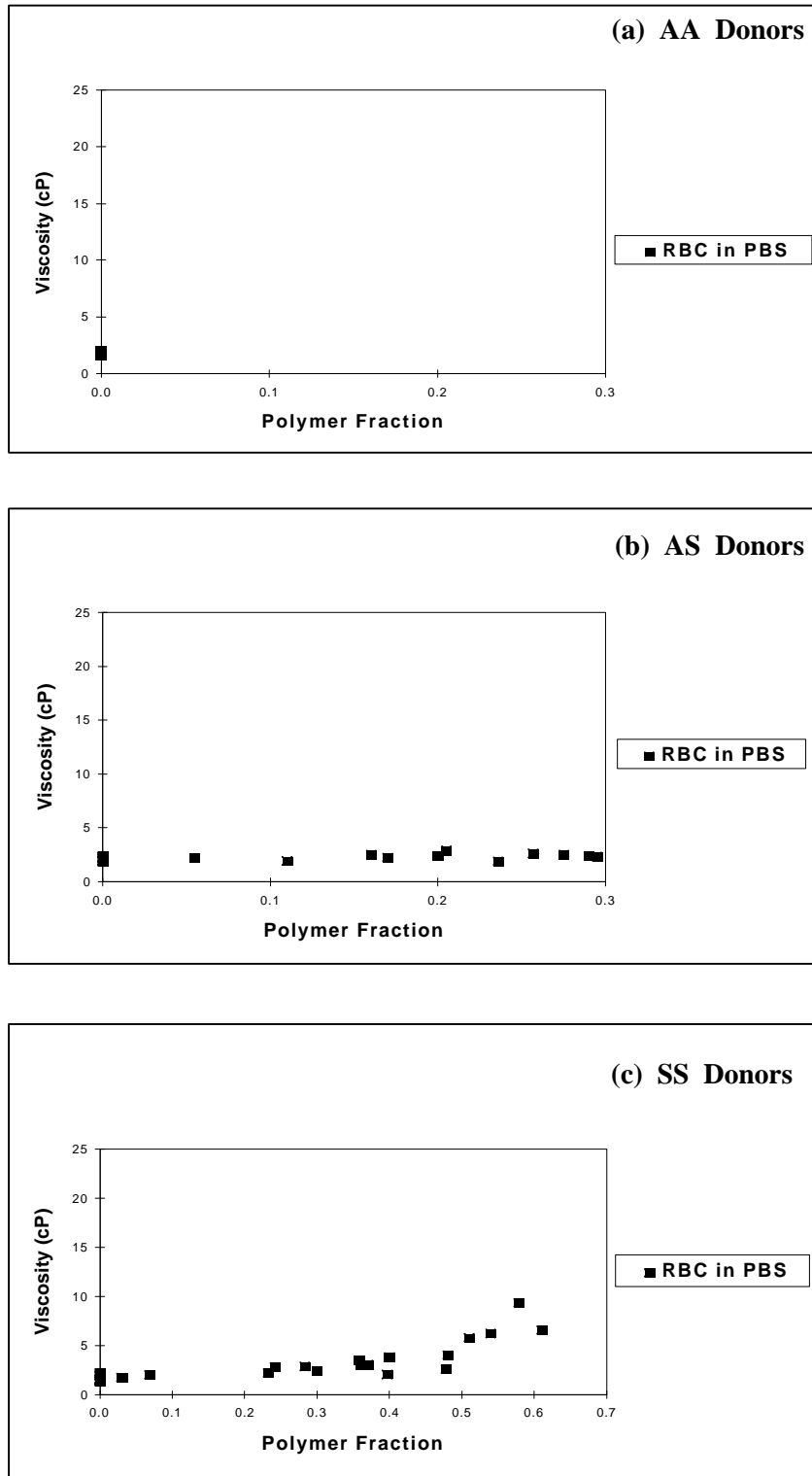


Figure 4.7: Apparent Viscosity vs. Polymer Fraction:  
 (a) AA donors, (b) AS donors, and (c) SS donors.

#### 4.4. Hemoglobin Solutions in Plasma

Hemoglobin solutions were obtained from 25 % red blood cell suspensions in plasma, using an ultrasonic sonicator. Before lysing the cells, the suspensions were exposed at ambient air, for more than an hour, for total oxygenation. Apparent viscosity results versus  $PO_2$  and  $SO_2$  are shown in Figs. 4.8, and 4.9. Normal donors show a constant linear relationship for both  $PO_2$  (Fig. 4.8.a) and  $SO_2$  (Fig. 4.9.a) curves, confirming that no major changes are noticed for normal blood viscosity upon deoxygenation. Sickle trait individuals still exhibit a very flat relationship, down to  $PO_2$  about 20 mmHg (Fig. 4.8.b). Below that critical level, the relationship tends to become steeper. The relationship between viscosity and  $SO_2$  (Fig. 4.9.b) is found to be linear (correlation factor is 0.62). Sickle cell individuals present very similar results, except that a more pronounced increase is observed still for  $PO_2$  below 40 mmHg (Fig. 4.8.c). The best curve fit for  $PO_2$  (Fig. 4.8.c) and  $SO_2$  (Fig. 4.9.c) curves are both logarithmic (correlation coefficients: 0.76 and 0.79, respectively, to compare with a linear regression: 0.44, and 0.68). The apparent viscosity results versus polymer fraction are shown in Fig. 4.10. For normal donors, there is still no polymer formation (Fig. 4.10.a). For sickle trait donors, a linear relationship was found up to 30 % polymer fraction (Fig. 4.10.b). Sickle cell individuals data (steady-state viscosity vs. polymer fraction) are presented in Fig. 4.10.c.

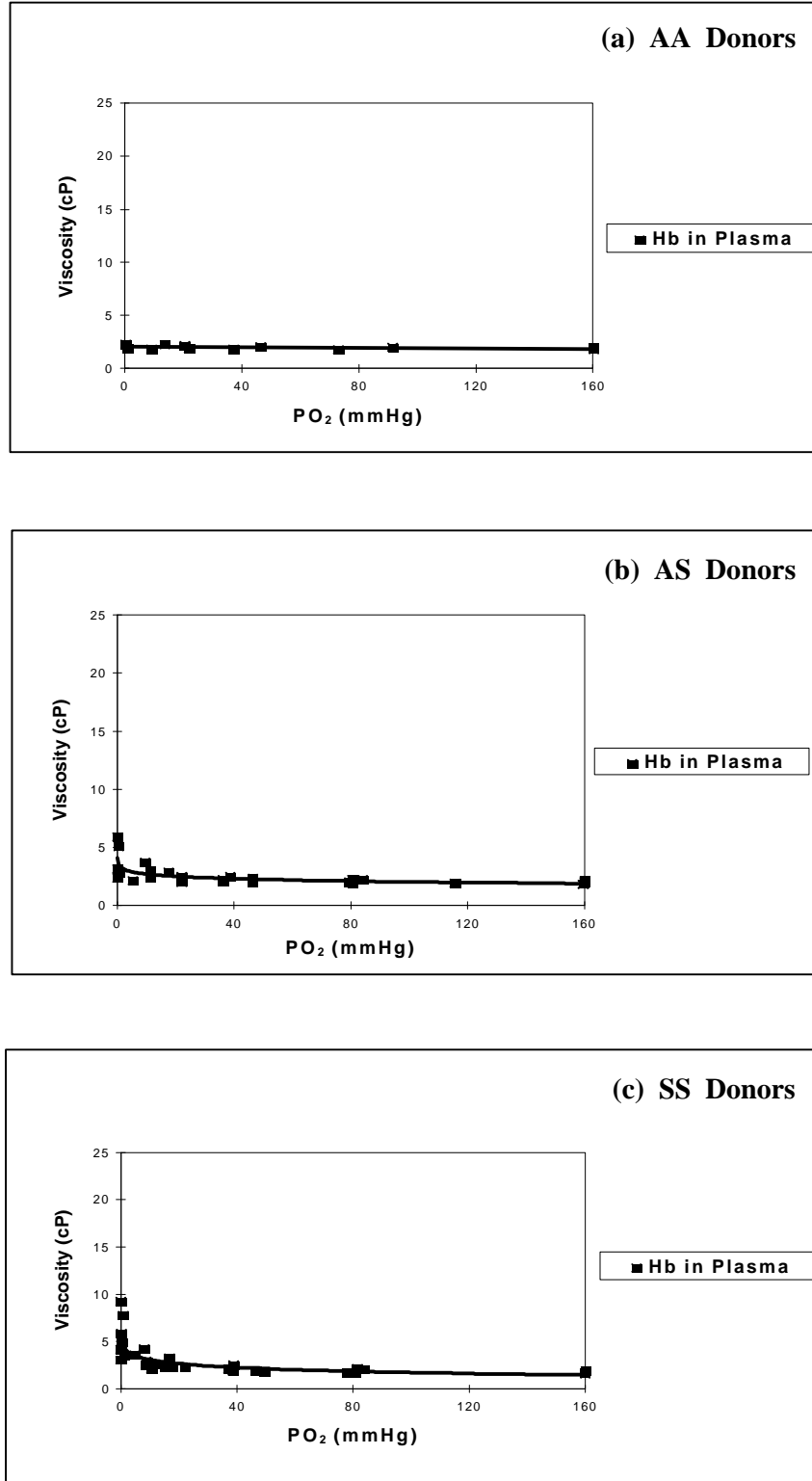


Figure 4.8: Apparent Viscosity vs. PO<sub>2</sub>:  
(a) AA donors, (b) AS donors, and (c) SS donors.

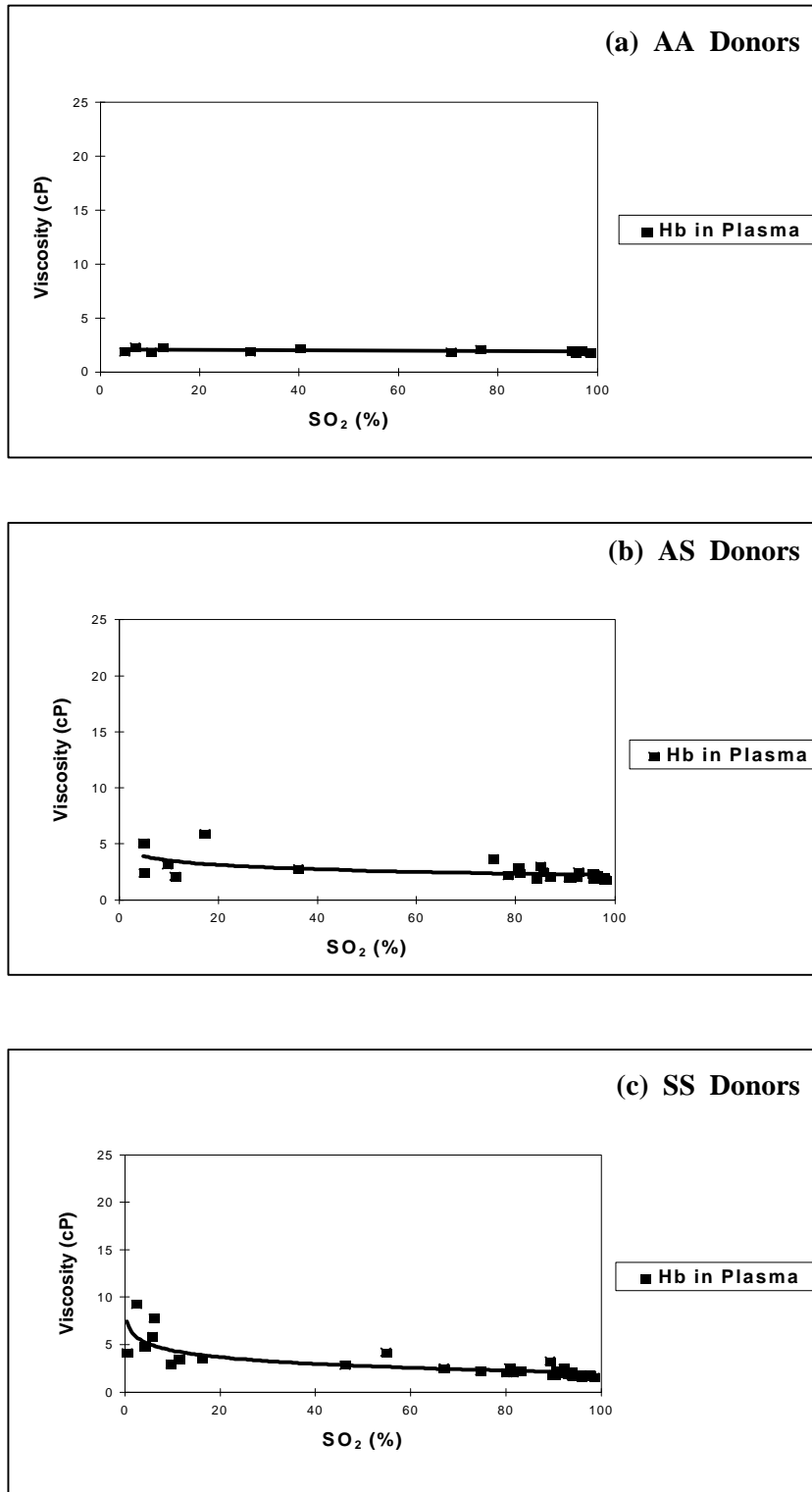


Figure 4.9: Apparent Viscosity vs.  $\text{SO}_2$ :  
(a) AA donors, (b) AS donors, and (c) SS donors.

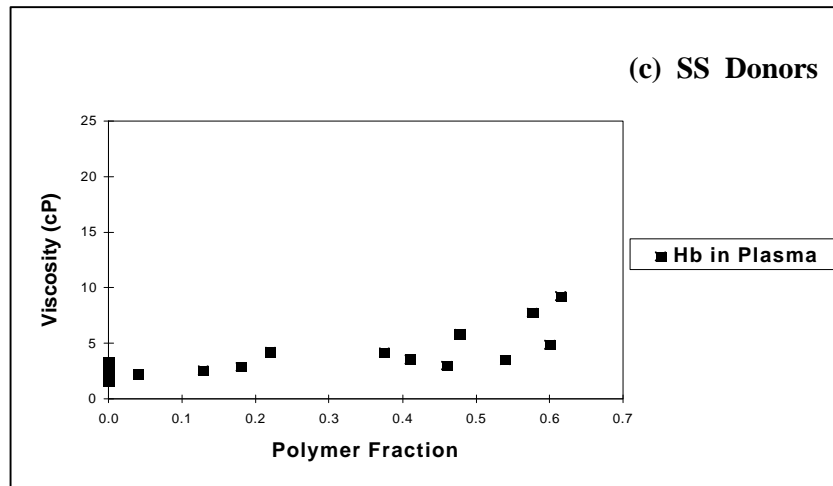
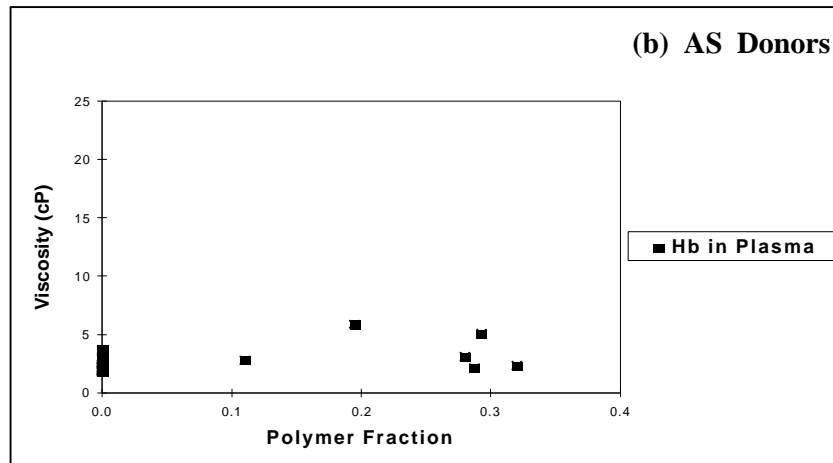
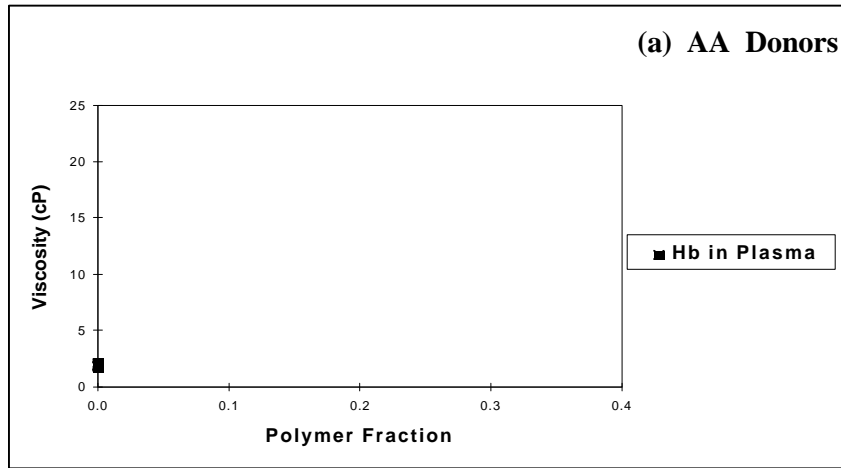


Figure 4.10: Apparent Viscosity vs. Polymer Fraction:  
 (a) AA donors, (b) AS donors, and (c) SS donors.

## CHAPTER 5 DISCUSSION

### 5.1. Blood Analysis

From the blood analysis (Table 4.1) normal donors have a majority of hemoglobin A (98-99 %) and traces of hemoglobin A<sub>2</sub>/C. No polymer formation occurs since sickle hemoglobin is totally absent (Figs. 4.4.a, 4.7.a, and 4.10.a).

Sickle trait is treated like a benign hemoglobin disorder disease. Donors with sickle trait undergo clinical complications only under extreme hypoxia. However, extreme variations in clinical expressions and complications among different sickle trait donors or even in the same individual [Cooper and Toole, 1972] are found, and remain unexplained even nowadays. Greater variability in blood viscosity is usually found in heterozygous sickle (AS) individuals where the average percentage of sickle hemoglobin is 40 % (range from 22 to 45 %, documented in the literature [Fibach et al., 1993]). However, as shown in Table 4.3, the present population studied is relatively homogenous (sickle hemoglobin:  $38.0 \pm 3.3$  %, normal hemoglobin:  $59.7 \pm 3.6$  %), which explains the similar polymer fraction profiles obtained for sickle trait individuals (Fig. 4.1), and fairly uniform values in the measurements.

Greater scatter in the hemoglobin measurements is found in homozygous sickle (SS) individuals. Average percentages are found to be  $84.8 \pm 12.5$  % sickle for hemoglobin and  $8.0 \pm 11.7$  % for fetal

hemoglobin (Table 4.3). Two donors were treated on Hydroxyurea (donors 6 and 9), which is an inhibitor of DNA synthesis. Hydroxyurea increases fetal hemoglobin levels in sickle cell individuals [Fibach et al., 1993; Rodgers et al., 1993], and to a lower degree in sickle  $\beta$  Thalassemia individuals. Hydroxyurea inhibits the polymerization process and tends to reduce vaso-occlusive occurrences. Therefore, the predicted polymer fraction curves for these two individuals, as shown in Fig. 4.1 are beneath the profiles of patients 7 and 8. Donor 9, with 26 % fetal hemoglobin and 73 % sickle hemoglobin has a calculated polymer fraction profile similar to sickle trait's donors. However, for this case polymer formation starts at 70 % oxygen saturation as opposed to 50 % in AS donors.

## 5.2. Study of Deoxygenation on Cell Rheology

Blood viscosity depends on many factors [Ditenfass, 1976]:

- metabolic,
- cancer,
- infections,
- trauma,
- genetic,
- immunological,
- emotional stress,
- drugs,
- some unknown factors (obesity and diet).

However, for sickle cell anemia the most important factors are:

1. hematocrit,
2. temperature,
3. amount of polymer inside the cell, which is a function of oxygen saturation, as well as a function of the hemoglobin composition and concentration,
4. alignment of polymer,
5. the proportions of dense cells and also Irreversible Sickled Cells (ISC),



6. transfusion,
7. membrane abnormalities,
8. cell-to-cell adhesion,
9. hemoglobin-membrane interactions,
10. serum proteins, pH,
11. haplotypes.

The scatter in the data is therefore a direct cause of the combination of some of these factors, factors that are sometimes hard to track down. In the protocol followed for this study, the effects of hematocrit and temperature are inhibited, since all the red blood cell suspensions are resuspended at 25 % hematocrit, and the temperature is maintained at 37°C. The pH is set to 7.4, by controlling the partial pressure in CO<sub>2</sub>, at 5.6 %. Haplotypes are not believed to be really influent, and therefore can be considered as a negligible factor. The effects of plasma proteins can be investigated, since measurements for red blood cell suspensions in both autologous plasma and Phosphate Buffer Solution are made. The amount of polymer formed inside the cell is predicted, and related to the partial pressure in oxygen, oxygen saturation, and viscosity measurements. If studying whole red blood cell suspensions appears to be relevant from a clinical point of view, one must keep in mind, that factors 4 to 9 may be important and need to be characterized. Dense cells have a dominant role into the sickling process [Hiruma et al., 1995], and this explains tremendous differences in polymer fractions at low levels in oxygen from one patient to another. Cell-to-cell adhesion, facilitated by plasma proteins [Hebbel, 1991] is also a factor that causes an increase in viscosity. Sickle cell individuals may present different combinations of these factors, which all are related somehow to the rheological properties of the red blood cells, and consequently have effects on viscosity measurements.

As discussed in Chapter 4, no theoretical model exists to express the viscosity as a function of polymer fraction (PF). Figure 5.1 summarizes the data of viscosity versus polymer fraction for normal, sickle trait, and sickle cell donors (suspensions in plasma, Phosphate Buffer Solution, and hemoglobin solutions). The corresponding linear regressions for polymer fraction below 55 % give the following results:

- SS RBC in Plasma:  $\eta = 7.936 \times PF + 2.713,$
- AS RBC in Plasma:  $\eta = 6.238 \times PF + 2.712,$
- SS RBC in PBS:  $\eta = 4.456 \times PF + 1.620,$
- AS RBC in PBS:  $\eta = 1.342 \times PF + 2.103.$

The increase in viscosity is linear with polymer fraction in sickle trait and in sickle cell individuals, as polymer fraction increases to 30 %. The linear relationship between viscosity suspensions and polymer goes on in sickle cell individuals up to a critical polymer fraction value of 50-55 %, as it is shown in Fig. 5.1. Above this critical value, a sharp increase in viscosity is seen. Red blood cell suspensions in plasma and in PBS are studied, in order to see if plasma proteins have any effects on the mechanical properties of red blood cells upon deoxygenation and to confirm the findings of Chien et al. [1970] and Usami et al. [1975].

From Fig. 5.1 it can be seen that the difference in viscosity between PBS and plasma results is due to the fact that the viscosity of plasma is slightly greater than the viscosity of PBS. The difference in viscosity disappears when the results in PBS are adjusted for the higher viscosity value of plasma under fully oxygenated condition (Fig. 5.2).

The linear regression for all the data gives

- for  $PF \leq 55 \%$   $\eta = 4.922 \times PF + 2.705,$
- for  $PF > 55 \%$   $\eta = 118.380 \times PF - 58.46.$

During these experiments, pH was also monitored. Starting around 7.4 at normal oxygen concentration (ambient air), the pH slightly increased at very low oxygen levels, to reach values around 7.6 in PBS and 7.8 in plasma. A small increase in pH is not expected to produce a significant change in viscosity.

Based on this work, apparent viscosity appears to be a potential good parameter for assessing clinical severity in sickle cell anemia. A complete characterization of viscosity as a function of polymer fraction is useful. Polymer fraction is a direct measurement of the polymerization process, but it is easier to measure viscosity than polymer fraction. Clinical severity in sickle cell patients can be accurately and quickly estimated, daily if necessary. This would allow a better tracking of the development of the disease, and also would permit to investigate the effects of some pharmacological agents.

### 5.3. Further Work

The present study is a step into the characterization of the rheological properties of sickle red blood cells. Below, is a list of observations and suggestions that should be considered in order to improve our understanding of the biorheological behavior of red blood cells.

1. A dynamic study should be done to express the elastic and viscous components as a function of polymer fraction for sickle trait and sickle cell individuals. This work will bring additional information, and could be a better parameter for assessing clinical severity or effects of drugs.

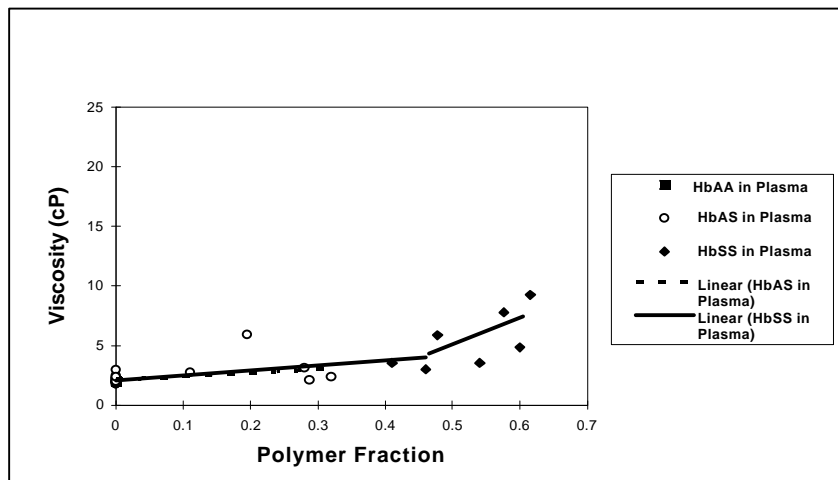
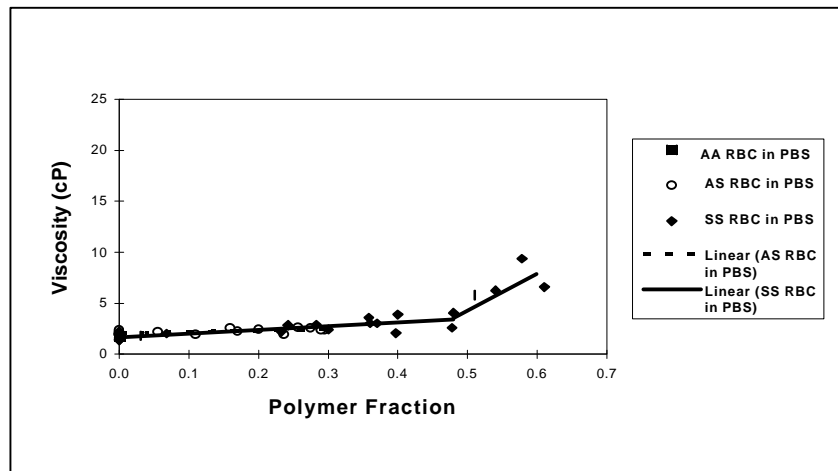
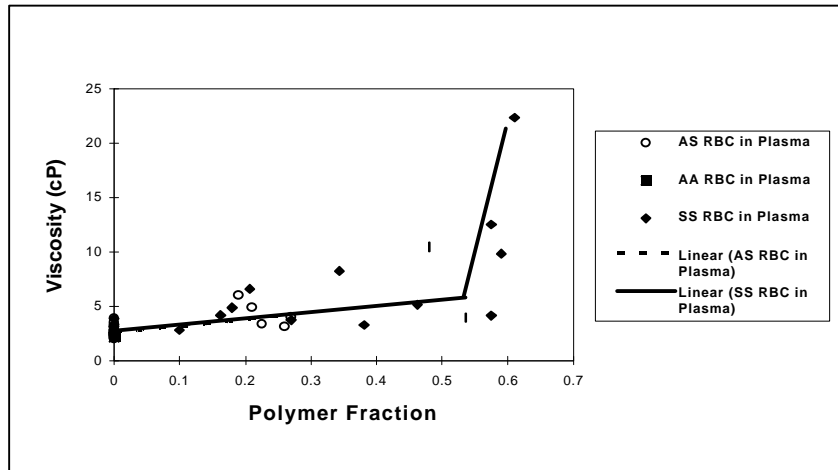


Figure 5.1: Best Curve Fits:  
Apparent Viscosity vs. Polymer Fraction  
(a) RBC in Plasma, (b) RBC in PBS, and (c) Hb in Plasma.

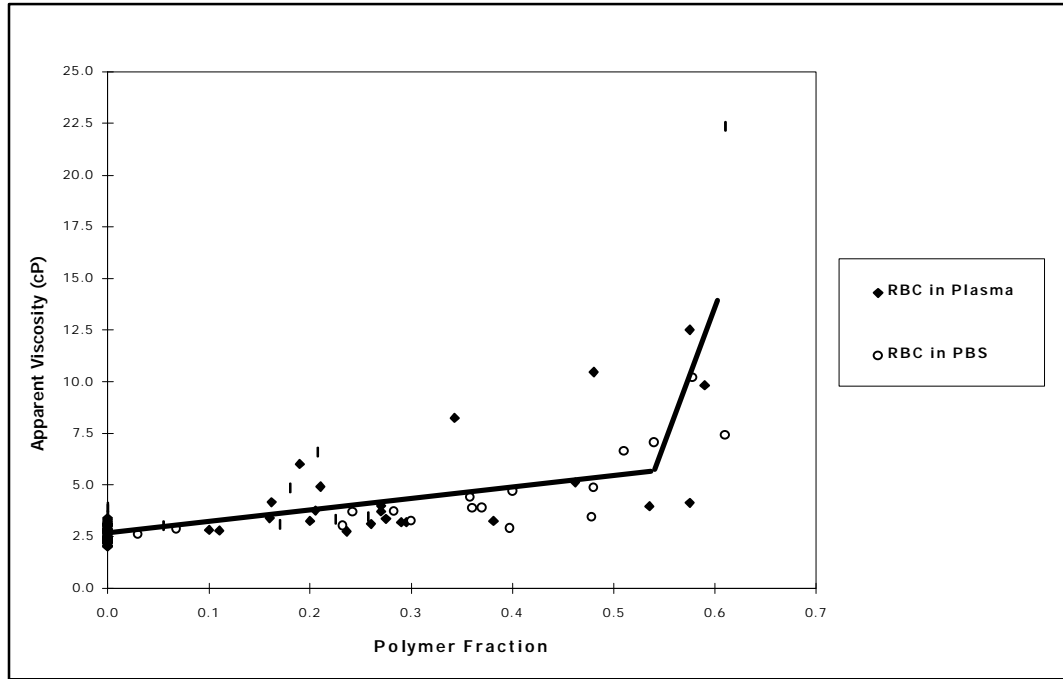


Figure 5.2: Best Curve Fit:  
Apparent Viscosity vs. Polymer Fraction:  
SS, AS RBC in Plasma and PBS.

2. It was shown in Chapter 2: Material and Methods, that it is easy to obtain hemoglobin from red blood cell suspensions. The problem with utilizing hemoglobin solutions, is that it is difficult to obtain hemoglobin concentrations as high as in cells. Therefore, the effects of deoxygenation on such suspensions are hard to interpret. It is suggested that hemoglobin solutions, and whole blood suspensions be studied in parallel, at higher hematocrit (ideally at 100 % hematocrit). Effects of deoxygenation would be studied on these solutions to determine the role of the cell membrane in the rheological measurements. Polymer fraction would be related to the steady-state and complex viscosities, both for AS, and SS individuals.

3. It would be interesting to find if the instrument is sensitive enough for studying the interactions between:

- RBC and endothelial cells,
- RBC and protein-coated (e.g. collagen) walls.

4. The effects of pharmacological agents on the kinetics and extent of hemoglobin gel formation should be studied.

## APPENDIX A

### TIME-TO-VOLTAGE CONVERSION

#### Time-to-Voltage Converter

Three major functional blocks characterize the Time-to-Voltage Converter (Model TVC 501, Tektronix, Florida): the front panel, the processor board and the counter board.

The front panel provides the user interface. Keyboard encoder data outputs to the processor board. Status and measurement data from the processor board inputs to the display controller and displayed by the front panel LEDs.

The processor board consists of the microprocessor, signal inputs circuits and power regulators. Its primary functions is to provide general instrument control and to generate triggers from the input signals. The microprocessor outputs measurements and status data to the front panel display controller. It also outputs data to a dual DAC. Each DAC output drives an AOP that produces the threshold level for a trigger comparator (Channels A and B). It shifts serial data, consisting of control bits and counter status bits, into a chain of shift registers. The shift register on the processor board outputs control bits for various processor board circuits. Shift registers on the counter board provide control bits, counter status bits and counter preload data. The signal inputs (Channels A and B) are connected to coupling switches (DC or AC). The switch outputs are sent to amplifier

circuits and then to trigger comparators where the trigger slope and level are set. The trigger comparator outputs go to the monitor outputs and the counter circuit board. The channel B is available in divide-by 100 and divide-by 1000. Several demonstration signals are available through the channel B monitor. The processor board supply the following voltages: +5 VA, +5 VAD, +12 VA, -12 VA, +21 V using the source voltage of the power module.

The counter board consists of the clock generator, pulse forming and synchronizing circuits, dual counter, DAC circuits and shift registers. This board performs Time-to-Voltage Conversions based on the duration of the input triggers. The counter board also generates test signals available at the channel B monitor output. The clock generator is the master clock that drives the pulse forming and synchronizing circuits. The trigger comparator outputs are inputs to the pulse forming and synchronizing circuits. The triggers are formed into a pulse representing the time interval to be measured. This time interval pulse is synchronized to the clock generator. When the time interval pulse is active, clock pulses are ANDed with it to form a burst. This burst is passed to the Dual counter. This last counts the number of pulses received in the clock burst from the pulse forming and synchronizing circuit. One bank select signal determines which bank is enabled for counting. The pulse count is loaded into the DAC. The DAC converts the count value into a corresponding current. An amplifier following the DAC produces an output voltage from the DAC current. The resulting voltage is the Time-to-Voltage Conversion.



An adjustment circuit including gain and offset potentiometers provides offset and gain calibration for the amplifier output.

The serial data from the processor board is shifted into a chain of shift registers and then back to the microprocessor. Data from the dual counter and status data is loaded into one set of registers. The microprocessor uses this data for the AUTO offset function. The processor can send a counter preload value to another set of registers. This preload value represents the offset value.

#### Voltage-to-Time Conversion and Time-to-Distance Conversion

1. Voltage between:  $-V_{min}$  and  $+V_{max}$ ,
2. Voltage = Voltage +  $|V_{min}|$ ,
3. Voltage now between: [ $V_{max}$  and  $+|V_{min}|$ ] and zero,
4. Voltage = Voltage / ( $V_{max} + |V_{min}|$ ),
5. Voltage now between 0 and 1,
6. Voltage = Voltage x  $H_{top}$ ,

where  $H_{top} = (H_{Determined} - Ball\_Diameter) - H_{Bottom}$ ,

7. Voltage = Voltage +  $H_{Bottom}$

where  $H_{Bottom} = 0.5 \times (TF - TVC) \times Speed\_of\_Sound\_Sample$ ,

where TF = Time of Flight, and TVC = Time to Voltage Converter Time.

## APPENDIX B

### CO-OXIMETER

The co-oximeter (Model AVOXimeter 1000, Avox Systems, Texas)

measures:

1. The saturation in oxygen (%HbO<sub>2</sub>),
2. The total hemoglobin concentration (THb),
3. The oxygen content (O<sub>2</sub> Content).

According to Beer's law, if several light-absorbing compounds are present in a solution, the concentration of each compound can be deducted if the compounds differ in their optical absorbencies and if optical density is measured at as many wavelengths as there are compounds present.

If 3 compounds X, Y, Z are present and if the optical density (OD) is measured at 3 different wavelengths ( $\lambda_i$ ), the result is a set of simultaneous equations with as many equations as there are unknown concentrations ( $c_i$ ). Thus, if the optical pathlength (l) and the extinction coefficient ( $\epsilon$ ) are known, the concentrations  $C_x$ ,  $C_y$ ,  $C_z$  can be computed from this set of equations:

$$OD(\lambda_1) = \epsilon_{x\lambda_1} \cdot C_x \cdot l + \epsilon_{y\lambda_1} \cdot C_y \cdot l + \epsilon_{z\lambda_1} \cdot C_z \cdot l$$

$$OD(\lambda_2) = \epsilon_{x\lambda_2} \cdot C_x \cdot l + \epsilon_{y\lambda_2} \cdot C_y \cdot l + \epsilon_{z\lambda_2} \cdot C_z \cdot l$$

$$OD(\lambda_3) = \epsilon_{x\lambda_3} \cdot C_x \cdot l + \epsilon_{y\lambda_3} \cdot C_y \cdot l + \epsilon_{z\lambda_3} \cdot C_z \cdot l$$

The AVOXimeter 1000 is capable of measuring the parameters listed above in a sample of whole blood, partially hemolysed and in hemoglobin

solutions. Five wavelengths are being used to obtain accurate measurements of the oxyhemoglobin saturation (%HbO<sub>2</sub>) and can detect four different hemoglobin species (oxyhemoglobin, deoxyhemoglobin, methemoglobin, carboxyhemoglobin). The oxyhemoglobin saturation is defined as follows:

$$\%HbO_2 = \frac{[HbO_2]}{[THb]}$$

$$[THb] = [HbO_2] + [Hb] + [MetHb] + [HbCO]$$

where

%HbO <sub>2</sub>	: Oxyhemoglobin saturation
[THb]	: Total hemoglobin concentration
[HbO <sub>2</sub> ]	: Oxyhemoglobin
[Hb]	: Deoxyhemoglobin
[MetHb]	: Methemoglobin
[HbCO]	: Carboxyhemoglobin

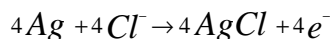
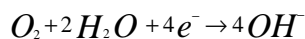
The accuracy is ± 1% for the measure of saturation in oxygen and respectively 0.45 g/dL (THb > 10 g/dL) and 0.35 g/dL (THb < 10 g/dL) for the measure of the total hemoglobin concentration.

## APPENDIX C

### OXYGEN MICROSENSOR

The chemical microsensor (Model 1231, Diamond General Development Corporation, Michigan) is capable of measuring the partial pressure in oxygen. A PO<sub>2</sub> polarographic sensing electrode (Model 757 oxygen needle electrode, Diamond General Development Corporation) will be used to check on the partial pressure in oxygen of the blood samples.

The oxygen needle electrode contains a cathode and an anode (reference electrode). When it is correctly polarized in a solution containing electrolytes and dissolved oxygen, current will flow as a result of the reduction of oxygen at the cathodic surface (negatively polarized). The reactions at the cathode and anode are respectively expressed as



The voltage-current relationship for a polarographic oxygen electrode is represented by the characteristic curve as shown in Figure 2.6 (Chapter 2: Materials and Methods). In the region around -0.7 Volt, the current tends to reach a plateau in which changes in voltage have little effect on current. In this plateau region, the current is limited by the rate at which oxygen can diffuse to the cathode. As the voltage is increased above -1.0 volt (or decreased below -0.5 Volt), the

current again increases (or decreases) with voltage due to the reduction of other elements in addition to oxygen.

The diffusion rate is a function of the oxygen diffusion coefficient of the membrane, media surrounding the cathode and the dissolved oxygen concentration. In turn, it is proportional to the oxygen partial pressure and temperature. Therefore, for a constant temperature ( $\pm 0.2$  degree Celsius), current flow through the electrode is directly proportional to the partial pressure in oxygen.

## APPENDIX D

### PROGRAM DESCRIPTIVE OF DATA ACQUISITION CODE

#### INTRODUCTION

The data acquisition code was written in Turbo Pascal 7.0 (Version Borland 7.0), composed of 14 independent units. This program runs on PC base (PC/XT/AT or above) and does not require any numerical co-processor (8087).

#### CODE INFORMATION

Source Compiled:	6245 lines.
Code size:	113904 bytes.
Data size:	36374 bytes.
Stack size:	16384 bytes.
Data size required for I/O:	655360 bytes.
No EMS required.	

#### UNITS

<i>PROJECT</i> (Main):	15 lines, Executable file, PROJECT.EXE.
<i>CONSULT</i> :	935 lines, Consultation of Patient's information and Viscoelastic measurements.
<i>COURBE10</i> :	275 lines, Plot curves on screen pixel by pixel.
<i>FB</i> :	185 lines, Run falling ball experiment.
<i>GRAPHIQU</i> :	325 lines, Contains diverse graphic subroutines for Input/Output operations in graphic mode and drawing subroutines.
<i>OSCB</i> :	355 lines, Run: - oscillating ball experiment, - GDM viscometry.

*OSCILLOS:* 2430 lines,  
 Drive the digitizing oscilloscope (Modes Listen/Talk).  
 Initialize digitizing oscilloscope parameters.  
 Take care of all the data transfers.  
 Order data transfer when needed.  
 Derive the viscosity from the data acquired.  
 Save the data into files.  
 Unit required for speed of sound, falling ball,  
 oscillating ball experiments and GDM viscometry.

*PARAMET:* 210 lines,  
 Initialize global parameters such as radius of the  
 ball, wall correction factor, capillary tube  
 diameter, height of oscillation...

*PATIENT:* 250 lines,  
 Allow the operator to enter all the patient's  
 information as well as information regarding the  
 ongoing experiment.

*SOS:* 105 lines,  
 Run speed of sound experiment.  
 Derive the exact height of the capillary tube.

*START:* 320 lines,  
 Main screen.  
 Initialize acquisition parameters and clear all  
 temporary data used to prepare the code for the  
 execution of a new run..  
 The operator can choose to:  
 - initialize global parameters,  
 - enter patient's information,  
 - consult stored information,  
 - run speed of sound,  
 - run falling ball,  
 - run oscillating ball or the GDM viscometer.

*STARTUP:* 145 lines,  
 Initialize all the variables, symbols and temporary  
 buffers for further use.  
 Select the optimal video mode and call the  
 unit START.

*TPDECL:* 475 lines,  
 Interface unit containing Input/Output subroutines  
 regarding the data transfer between the digitizing  
 oscilloscope, and the GPIB.

*VARIABLE:* 220 lines,  
 Contains all the definitions and declarations of:  
 - CONSTANTS,  
 - TYPES (record, file...)  
 - VARIABLES (real, pointer, file...).

FUNCTIONAL SCHEMATIC

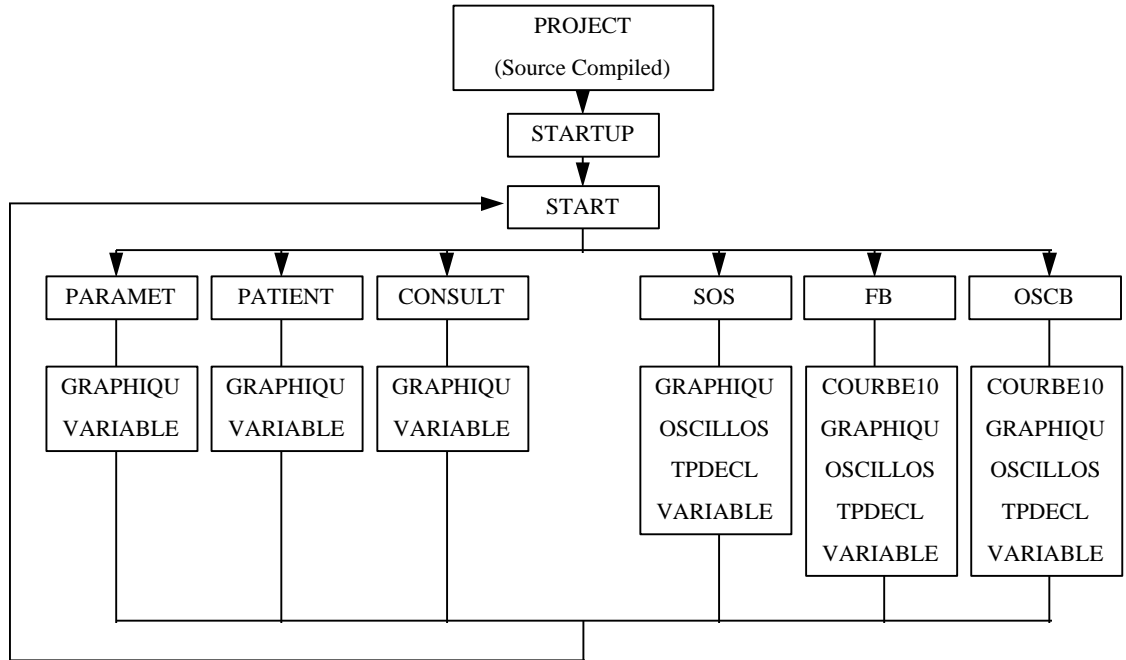


Figure D.1: Functional Schematic.



#### LIST OF REFERENCES

- Abraham, D.J., Mehanna, A.S., Wireko, F.C., Whitney, J., Thomas, R.P., and Orringer, E.P., 1991, "Vanillin, a Potential Agent for the Treatment of Sickle Cell Anemia," *Blood*, Vol. 77, No. 6, pp. 1334-1341.
- Briehl, R.W., and Nikolopoulou, P., 1993, "Kinetics of Hemoglobin S Polymerization and Gelation Under Shear: I. Shape of the Viscosity Progress Curve and Dependence of Delay Time and Reaction Rate on Shear Rate Temperature," *Blood*, Vol. 31, No. 9, pp. 2420-2428.
- Chien, S., King, R.G., Kaperonis, A.A., and Usami, S., 1982, "Viscoelastic Properties of Sickle Cells and Hemoglobin," *Blood Cells*, Vol. 8, pp. 53-64.
- Chien, S., Usami, S., and Bertles J.F., 1970, "Abnormal Rheology of Oxygenated Blood in Sickle Cell Anemia," *The Journal of Clinical Investigation*, Vol. 49, pp. 623-634.
- Coffey, B.E., 1991, "Effects of Temperature Cell Density and Various Clinical Treatments on the Rheology of Packed Suspensions of Normal Cells and Sickle Cells," Duke University, Ph.D. Dissertation.
- Cooper, M.R., and Toole, J.F., 1972, "Sickle-Cell Trait: Benign or Malignant?" *Annals of Internal Medicine*, Vol. 77, No. 6, pp. 997-999.
- Del Grosso, V.A., and Mader, C.W., 1972, "Speed of Sound in Pure Water," *J. Acoust. Soc. Amer.*, Vol. 52, pp. 1442-1446.
- Dintenfass, L., 1976, *Rheology of Blood in Diagnostic and Preventive Medicine*, Butterworths, London/Boston.
- Dintenfass, L., 1985, *Blood Viscosity, Hyperviscosity & Hyperviscosaemia*, MTP Press Limited, Boston.
- Dong, C., Chadwick, R.S, and Schechter, A.N., 1992, "Influence of Sickle Hemoglobin Polymerization and Membrane Properties on Deformability of Sickle Erythrocytes in the Microcirculation," *Biophys. J.*, Vol. 63, pp. 774-783.
- Evans, E.A., and Mohandas, N., 1987, "Membrane-Associated Sickle Hemoglobin: A Major Determinant of Sickle Erythrocyte Rigidity," *Blood*, Vol. 70, No. 5, pp. 1443-1449.
- Fibach, E., Burke, L.P., Schechter, A.N., Noguchi, C.T., and Rodgers, G.P., 1993, "Hydroxyurea Increases Fetal Hemoglobin in Cultured Erythroid Cells Derived From Normal Individuals and Patients With Sickle Cell Anemia or  $\beta$  Thalassemia," *Blood*, Vol. 81, No. 6, pp. 1630-1635.

- Gilinson, P.J., Dauwalter, C.R., and Merrill, E.W., 1963, "A Rotational Viscometer Using an A.C. Torque to Balance Loop and Air Bearing," *Transactions of the Society of Rheology*, Vol. 7, pp. 319-331.
- Gill, S.J., Spokane, R., Benedict, R.C., and Fall, L., 1980, "Ligand-linked Phase Equilibrium of Sickle Cell Hemoglobin," *J. Mol. Biol.*, Vol. 140, pp. 299-312.
- Hasegawa, S., Hiruma, H., Uyesaka, N., Noguchi, C.T., Schechter, A.N., and Rodgers, G.P., 1995, "Filterability of Mixtures of Sickle and Normal Erythrocytes," *American Journal of Hematology*, Vol. 50, pp. 91-97.
- Hebbel, R.P., 1991, "Beyond Hemoglobin Polymerization: The Red Blood Cell Membrane and Sickle Disease Pathophysiology," *Blood*, Vol. 77, No. 2, pp. 214-237.
- Hiruma, H., Noguchi, C.T., Uyesaka, N., Hasegawa, S., and Blanchette-Mackie, E.J., 1995, "Sickle Cell Rheology Is Determined by Polymer Fraction--Not Cell Morphology," *American Journal of Hematology*, Vol. 48, pp. 19-28.
- Hiruma, H., Noguchi, C.T., Uyesaka, N., Schechter, A.N., and Rodgers, G.P., 1995, "Contributions of Sickle Hemoglobin Polymer and Sickle Cell Membranes to Impaired Filterability," *Am. J. Physiol.*, Vol. 268, pp. H2003-H2008.
- Hochmuth, R.M., 1993, "Measuring the Mechanical Properties of Individual Human Blood Cells," *Journal of Biomechanical Engineering*, Vol. 115, pp. 515-519.
- Hofrichter, J., 1979, "Ligand Binding and the Gelation of Sickle Cell Hemoglobin," *J. Mol. Biol.*, Vol. 128, pp. 335-369.
- Holman, J.P., and Gajda, W.J., 1984, *Experimental Methods for Engineers*, 4th Edition, McGraw-Hill Book Company, New York.
- Itoh, T., Chien, S., Usami, S., 1992, "Deformability measurements on individual sickle cells using a new system with PO<sub>2</sub> and temperature control," *Blood*, Vol. 79, No. 8, pp. 2141-2147.
- Johnson, R.M., Acquaye, C., Feo, C., and Sarnaik, S., 1994, "Bepiridil as an Antisickling Agent: Membrane Internalization and Cell Rigidity," *American Journal of Hematology*, Vol. 46, pp. 310-318.
- Landau, L., and Lifshitz, E., 1971, *Mécanique des Fluides*, Editions MIR, Moscow.
- Mackie, L.H., and Hochmuth, R.M., 1990, "The Influence of Oxygen Tension, Temperature, and Hemoglobin Concentration on the Rheological Properties of Sickle Erythrocytes," *Blood*, Vol. 76, No. 6, pp. 1256-1261.
- Minton, A.P., 1977, "Non-ideality and Thermodynamics of Sickle-cell Hemoglobin Gelation," *J. Mol. Biol.*, Vol. 110, pp. 89-103.
- Morris, C.L., Rucknagel, D.L., and Joiner, C.H., 1993, "Deoxygenation Induced Changes in Sickle Cell-Sickle Adhesion," *Blood*, Vol. 81, No. 11, pp. 3138-3145.

- Noguchi, C.T., 1984, "Polymerization in Erythrocytes Containing S and Non-S Hemoglobins," *Biophys. J.*, Vol. 45, pp. 1153-1158.
- Noguchi, C.T., and Schechter, A.N., 1981, "The Intracellular Polymerization of Sickie Hemoglobin and Its Relevance to Sickie Cell Disease," *The Journal of The American Society of Hematology*, Vol. 58, No. 6, pp. 1057-1068.
- Noguchi, C.T., and Schechter, A.N., 1985, "Sickie Hemoglobin Polymerization Solution and in Cells," *Ann. Rev. Biophys. Chem.*, Vol. 14, pp. 239-263.
- Noguchi, C.T., Torchia, D.A, and Schechter, A.N., 1979, "C NMR Quantification of Polymer in Deoxyhemoglobin S Gels," *Proc. Natl. Acad. Sci. USA*, Vol. 76, No. 10, pp. 4936-4940.
- Noguchi, C.T., Torchia, D.A., and Schechter, A.N., 1980, "Determination of Deoxyhemoglobin S Polymer in Sickie Erythrocytes Upon Deoxygenation," *Proc. Natl. Acad. Sci. USA*, Vol. 77, No. 9, pp. 5487-5491.
- Noguchi, C.T., Torchia, D.A, and Schechter, A.N., 1981, "Polymerization of Hemoglobin in Sickie Trait Erythrocytes and Lysates," *The Journal of Biological Chemistry*, Vol. 256, pp. 4168-4171.
- Noguchi, C.T., Torchia, D.A., and Schechter, A.N., 1983, "Intracellular Polymerization of Sickie Hemoglobin--Effects of Cell Heterogeneity," *The Journal of Clinical Investigation*, Vol. 72, pp. 846-852.
- Reilly, M.P., Horiuchi, K., and Asakura, T., 1993, "Dose-Dependent Red Blood Cell Volume Increase Induced by Bepiridil," *Gen. Pharmac.*, Vol. 24, No. 6, pp. 1323-1329.
- Rodgers, G.P., Dover, G.J., Uyesaka, N., Noguchi, C.T., Schechter, A.N., and Nienhuis, A.W., 1993, "Augmentation by Erythropoietin of the Fetal-Hemoglobin Response to Hydroxyurea in Sickie Cell Disease," *The New England Journal of Medicine*, Vol. 328, No. 2, pp. 73-80.
- Rodgers, G.P., Noguchi, C.T., and Schechter, A.N., 1994, "Sickie Cell Anemia," *Scientific American Science & Medicine*, Vol. 1, No. 4, pp. 48-57.
- Rodgers, G.P., Schechter, A.N., and Noguchi, C.T., 1985, "Cell Heterogeneity in Sickie Cell Disease: Quantification of the Erythrocyte Density Profile," *J. Lab. Clin. Med.*, Vol. 106, No. 1, pp. 30-37.
- Schechter, A.N., and Noguchi, C.T., 1994, *Sickie Hemoglobin Polymer: Structure--Function Correlates, Sickie Cell Disease: Basic Principles and Clinical Practice*, Raven Press, Ltd., New York, pp. 33-51.
- Schmalzer, E.A., Lee, J.O., Brown, A.K., Usami, S., and Chien, S., 1987, "Viscosity of Mixtures of Sickie and Normal Red Cells at Varying Hematocrit Levels," *Transfusion*, Vol. 27, No. 3, pp. 228-233.
- Shung, K.K., Krisko, B.A., and Ballard, J.O., 1982, "Acoustic Measurement of Erythrocyte Compressibility," *J. Acoust. Soc. Amer.*, Vol. 72, pp. 1364-1367.

- Sunshine, H.R., Hofrichter, J., Ferrone, F.A., and Eaton, W.A., 1982, "Oxygen Binding by Sickle Cell Hemoglobin Polymers," *J. Mol. Biol.*, Vol. 158, pp. 251-273.
- Tran-Son-Tay, R., Beaty, B.B., Acker, D.N., and Hochmuth, R.M., 1988, "Magnetically Driven, Acoustically Tracked, Translating-Ball Rheometer for Small, Opaque Samples," *Rev. Sci. Instrum.*, Vol. 59, No. 8, pp. 1399-1404.
- Tran-Son-Tay, R., Nash, G.B., and Meiselman, H.J., 1986, "Oscillatory Viscometry of Red Blood Cell Suspensions: Relations to Cellular Viscoelastic Properties," *J. Rheology*, Vol. 30, pp. 231-249.
- Usami, S., Chien, S., Scholtz, P.M., and Bertles, J.F., 1975, "Effects of Deoxygenation on Blood Rheology in Sickle Cell Disease," *Microvascular Research*, Vol. 9, pp. 324-334.
- West, J.B., 1979, *Respiratory Physiology, The Essentials*, 2nd Edition, Williams & Wilkins, Baltimore.
- Zieman, F., Radler, J., and Sackman, E., 1994, "Local Measurements of Viscoelastic Moduli of Entangled Actin Networks Using an Oscillating Magnetic Bead Micro-Rheometer," *Biophysical Journal*, Vol. 66, pp. 2210-2216.

## BIOGRAPHICAL SKETCH

Born on February 13th, 1970, David Gilles Morio received his "Diplôme d'Ingénieur" in biomedical engineering from the University of Technology of Compiègne, France, in June 1995. His will to learn more and his desire to get experience from a stay in a foreign country led him to come for graduate work at the University of Florida at the Department of Aerospace Engineering, Mechanics, and Engineering Science in Fall 1994. He graduated with a Master of Science in engineering mechanics, in August 1996.

I certify that I have read this study and that in my opinion it conforms to acceptable standards of scholarly presentation and is fully adequate, in scope and quality, as a thesis for the degree of Master of Science.

---

Roger Tran-Son-Tay, Chair  
Associate Professor of Aerospace  
Engineering, Mechanics, and  
Engineering Science

I certify that I have read this study and that in my opinion it conforms to acceptable standards of scholarly presentation and is fully adequate, in scope and quality, as a thesis for the degree of Master of Science.

---

Ulrich H. Kurzweg  
Professor of Aerospace  
Engineering, Mechanics, and  
Engineering Science

I certify that I have read this study and that in my opinion it conforms to acceptable standards of scholarly presentation and is fully adequate, in scope and quality, as a thesis for the degree of Master of Science.

---

Robert J. Hirko  
Associate Engineer of Aerospace  
Engineering, Mechanics, and  
Engineering Science

This thesis was submitted to the Graduate Faculty of the College of Engineering and to the Graduate School and was accepted as partial fulfillment of the requirements for the degree of Master of Science.

August, 1996

---

Winfred M. Phillips  
Dean, College of Engineering

---

Karen A. Holbrook  
Dean, Graduate School